Progress In Electromagnetics Research, PIER 42, 49–89, 2003

STABILITY OF CLASSICAL FINITE-DIFFERENCE TIME-DOMAIN (FDTD) FORMULATION WITH NONLINEAR ELEMENTS — A NEW PERSPECTIVE

F. Kung and H. T. Chuah

Faculty of Engineering
Multimedia University
Jalan Multimedia
63100 Cyberjaya, Selangor, Malaysia

Abstract—In this paper new stability theorems for Yee's Finite-Difference Time-Domain (FDTD) formulation are derived based on the energy method. A numerical energy expression is proposed. This numerical energy is dependent on the FDTD model's E and H field components. It is shown that if the numerical energy is bounded, then all the field components will also be bounded as the simulation proceeds. The theorems in this paper are inspired by similar results in nonlinear dynamical system. The new theorems are used to prove the stability of a FDTD model containing non-homogeneous dielectrics, perfect electric conductor (PEC) boundary, nonlinear dielectric and also linear/nonlinear lumped elements. The theorems are intended to complement the well-known Courant-Friedrich-Lewy (CFL) Criterion. Finally it is shown how the theorems can be used as a test, to determine if the formulation of new lumped element in FDTD is proper or not. A proper formulation will preserve the dynamical stability of the FDTD model. The finding reported in this paper will have implications in the manner stability analysis of FDTD algorithm is carried out in the future.

1. INTRODUCTION

Classical Finite-Difference Time-Domain (FDTD) method using Yee's second order formulation [1] has been successfully employed to model a wide range of microwave circuits and high-frequency printed circuit board (PCB) assembly [2–5]. Traditionally to ensure numerical stability of the algorithm for a linear model, the Courant-Friedrich-Lewy (CFL) Criterion has to be fulfilled [3]. In an unstable algorithm the computed E and H field components will increase without limit as the simulation progresses. The CFL Criterion has been derived with the assumption of homogeneous linear dielectric and unbounded medium using Discrete Fourier Transform (DFT) (the Von Neumann approach, [6, 9]). For a practical microwave circuit model the CFL Criterion serves as a rule-of-thumb at best. A few attempts recently extended the stability analysis to include linear dispersive media [6] and linear lumped elements [7]. There is also an attempt to cast the FDTD method into iterative matrix equation [8]. The methods reported still rely on mathematical tools for linear systems (i.e., superposition principle, DFT etc.) and will fail for nonlinear models. To-date to the best of the authors' knowledge, there is still no satisfactory theory to explain the stability of FDTD formulation containing non-homogeneous dielectrics, boundary condition, nonlinear dielectric and also linear and nonlinear lumped elements arranged in an arbitrary manner. In this paper new stability theorems based on the energy method are derived to address the issue. This work is inspired by stability theory of dynamical systems [10], notably the Second Liapunov Method [11–13]. Although not shown due to lack of space, the FDTD formulation is actually a discrete dynamical system. The proof of the theorems is shown in Appendix A and B and the application is demonstrated in the main text. The theorem is used to prove what have been known throughout the years via simulation, that the incorporation of certain lumped components such

as resistor, capacitor, diode and bipolar junction transistor in the FDTD framework is found to be stable. The theorems also show with ease how a model containing non-homogeneous and nonlinear dielectric is stable. The theorems are intended to complement the CFL Criterion and the results of [6–8]. In Section 3 it is shown how the theorems are used as a test, to determine whether the inclusion of new lumped element in FDTD is proper without performing lengthy simulation. A proper formulation will preserve the stability of the FDTD model. We begin by considering a 3D FDTD model for PCB or microwave circuit without any source (voltage or current source), with perfect electric conductor (PEC) as the model boundaries. The new theorems are stated and we proceed to prove the stability of the sourceless model. Then we extend the theorems to check the stability of a 3D FDTD model with voltage source. Finally a simple simulation example serves to substantiate the results.

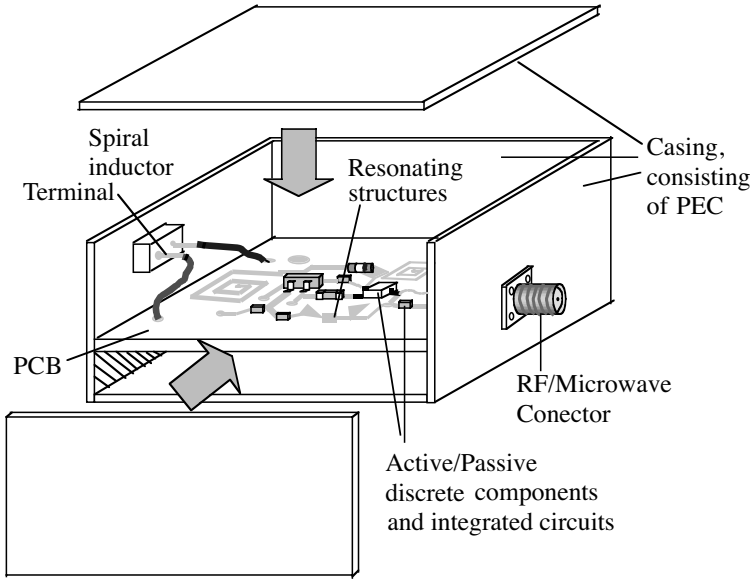

Figure 1. A typical microwave circuit module.

2. THE NEW STABILITY THEOREM

Figure 1 shows a typical 3D FDTD model for microwave circuit PCB without any voltage or current source, with perfect electric conductor (PEC) as the model boundaries. Discretization and field components of each Yee's Cell are shown in Figure 2. The model has n_x, n_y and n_z

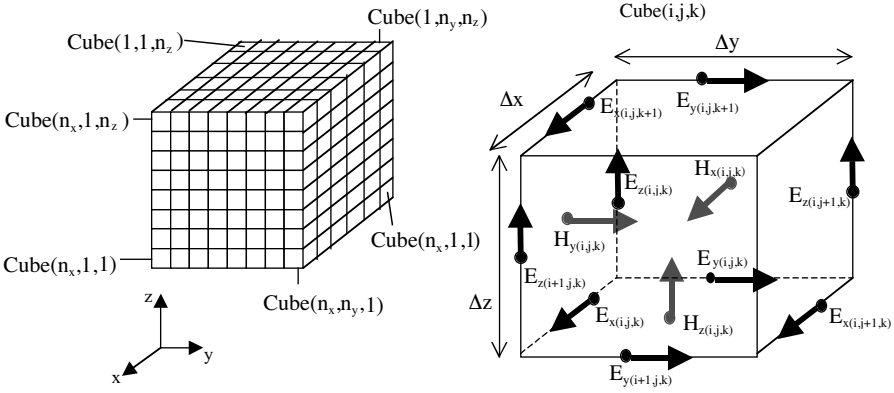

Figure 2. Discretization of the 3D mode, and the standard Yee's Cell (i, j, k) with associated field components.

cells along x, y and z axis respectively. Initially we assume the model to be non-magnetic, i.e., $\mu = \mu_o$ for all H fields. Also the cells are the same in size. All the E and H field components within the model have update equations given by the following form [3–5].

$$H^{n+\frac{1}{2}}_{x(i,j,k)} = H^{n-\frac{1}{2}}_{x(i,j,k)} - \frac{\Delta t}{\mu}\nabla \times E^{n}_{x(i,j,k)} \tag{1a}$$

$$H^{n+\frac{1}{2}}_{y(i,j,k)} = H^{n-\frac{1}{2}}_{y(i,j,k)} - \frac{\Delta t}{\mu}\nabla \times E^{n}_{y(i,j,k)} \tag{1b}$$

$$H^{n+\frac{1}{2}}_{z(i,j,k)} = H^{n-\frac{1}{2}}_{z(i,j,k)} - \frac{\Delta t}{\mu}\nabla \times E^{n}_{z(i,j,k)} \tag{1c}$$

$$E^{n+1}_{x(i,j,k)} = E^{n}_{x(i,j,k)} + \frac{\Delta t}{\varepsilon_{x(i,j,k)}}\left[\nabla \times H^{n+\frac{1}{2}}_{x(i,j,k)} - J^{n+\frac{1}{2}}_{x(i,j,k)}\right] \tag{1d}$$

$$E^{n+1}_{y(i,j,k)} = E^{n}_{y(i,j,k)} + \frac{\Delta t}{\varepsilon_{y(i,j,k)}}\left[\nabla \times H^{n+\frac{1}{2}}_{y(i,j,k)} - J^{n+\frac{1}{2}}_{y(i,j,k)}\right] \tag{1e}$$

$$E^{n+1}_{z(i,j,k)} = E^{n}_{z(i,j,k)} + \frac{\Delta t}{\varepsilon_{z(i,j,k)}}\left[\nabla \times H^{n+\frac{1}{2}}_{z(i,j,k)} - J^{n+\frac{1}{2}}_{z(i,j,k)}\right] \tag{1f}$$

where in (1a)–(1f)

$$\nabla \times E^{n}_{x(i,j,k)} = \frac{E^{n}_{z(i,j+1,k)} - E^{n}_{z(i,j,k)}}{\Delta y} - \frac{E^{n}_{y(i,j,k+1)} - E^{n}_{y(i,j,k)}}{\Delta z} \tag{1g}$$

$$\nabla \times H^{n+\frac{1}{2}}_{x(i,j,k)} = \frac{H^{n+\frac{1}{2}}_{z(i,j,k)} - H^{n+\frac{1}{2}}_{z(i,j-1,k)}}{\Delta y} - \frac{H^{n+\frac{1}{2}}_{y(i,j,k)} - H^{n+\frac{1}{2}}_{y(i,j,k-1)}}{\Delta z} \tag{1h}$$

and so forth for y and z terms. Notice that the restriction for ε has been removed, allowing it to vary according to location and orientation. Though not indicated, $\varepsilon_{r(i,j,k)}$ $(r = x, y, z)$ can also be functions of field components at previous time-steps. Similarly the current density term $J^{n+\frac{1}{2}}_{r(i,j,k)}$ $(r = x, y, z)$ also depends only on E and H field components at earlier time-steps.

Equations (1a)–(1f) will be known as the *Canonical FDTD Form* for E and H field components. Update equations for many applications can usually be written in this form. Let us now introduce two new quantities, as defined by:

$$V^n = \frac{\Delta V}{2} \sum_{k=1}^{n_z} \sum_{j=1}^{n_y} \sum_{i=1}^{n_x} \left[\begin{array}{l} \displaystyle\sum_{r=x,y,z} \left(\varepsilon_{r(i,j,k)} (E^n_{r(i,j,k)})^2 + \mu_o (H^{n-\frac{1}{2}}_{r(i,j,k)})^2 \right) \\ -H^{n-\frac{1}{2}}_{x(i,j,k)} \left[\dfrac{\Delta t}{\Delta y} \left(E^n_{z(i,j+1,k)} - E^n_{z(i,j,k)} \right) \right. \\ \qquad \left. - \dfrac{\Delta t}{\Delta z} \left(E^n_{y(i,j,k+1)} - E^n_{y(i,j,k)} \right) \right] \\ -H^{n-\frac{1}{2}}_{y(i,j,k)} \left[\dfrac{\Delta t}{\Delta z} \left(E^n_{x(i,j,k+1)} - E^n_{x(i,j,k)} \right) \right. \\ \qquad \left. - \dfrac{\Delta t}{\Delta x} \left(E^n_{z(i+1,j,k)} - E^n_{z(i,j,k)} \right) \right] \\ -H^{n-\frac{1}{2}}_{z(i,j,k)} \left[\dfrac{\Delta t}{\Delta x} \left(E^n_{y(i+1,j,k)} - E^n_{y(i,j,k)} \right) \right. \\ \qquad \left. - \dfrac{\Delta t}{\Delta y} \left(E^n_{x(i,j+1,k)} - E^n_{x(i,j,k)} \right) \right] \end{array} \right] \tag{2a}$$

$$P_d = -\Delta V \sum_{k=1}^{n_z} \sum_{j=1}^{n_y} \sum_{i=1}^{n_x} \left\{ \sum_{r=x,y,z} \frac{1}{2} \left(E^{n+1}_{r(i,j,k)} + E^n_{r(i,j,k)} \right) J^{n+\frac{1}{2}}_{r(i,j,k)} \right\} \tag{2b}$$

where $\Delta V = \Delta x \Delta y \Delta z$. In equation (2a), V^n is known as the 'numerical energy' of the 3D FDTD model at sequence n, it is analogous to the stored electromagnetic energy in a physical system. It comprises all the E field components at time-step n and H field components at time-step $n - \frac{1}{2}$. Similarly the numerical energy V^{n+1} comprises all E and H field components at time-step $n + 1$ and $n + \frac{1}{2}$ respectively. In (2b) each term $\frac{1}{2}(E^{n+1}_{r(i,j,k)} + E^n_{r(i,j,k)}) J^{n+\frac{1}{2}}_{r(i,j,k)}$ will be known as 'elemental dissipation' since it is the approximate power density dissipated by lumped element coinciding with $E_{r(i,j,k)}$ field.

The negative sum of all elemental dissipation multiplied by ΔV is the total dissipation P_d of the model. Since all the boundaries are PEC, the numerical energy within the model cannot escape from the boundary. The following theorems give the relationship between numerical energy and total dissipation, and the stability result.

Lemma 2.1 – Relationship between numerical energy and total dissipation

Consider a 3D FDTD model with PEC boundaries of Figure 1. Given that all field update equations are of the form (1a)–(1f), with V^n and P_d as defined in (2a) and (2b), then the following relation is true:

$$V^{n+1} - V^n = \Delta t \cdot P_d \qquad \square \quad (3)$$

Lemma 2.2 – Positive definiteness of V^n

Consider a 3D FDTD model with PEC boundaries of Figure 1. Given that all field update equations are of the form (1a)–(1f), then V^n is positive definite if and only if:

(a) $\varepsilon_{x(i,j,k)} > 0,\ \varepsilon_{y(i,j,k)} > 0,\ \varepsilon_{z(i,j,k)} > 0$ and $\mu = \mu_o > 0.$ (4a)

(b) For $\varepsilon = \min\{\varepsilon_{x(i,j,k)}, \varepsilon_{y(i,j,k)}, \varepsilon_{z(i,j,k)}\}$ and $c_m = \frac{1}{\sqrt{\mu_o \varepsilon}}$, let:

$$\Delta t < \min\left\{ \frac{1}{c_m\sqrt{2}\sqrt{\frac{1}{\Delta y^2}+\frac{1}{\Delta z^2}}}, \frac{1}{c_m\sqrt{2}\sqrt{\frac{1}{\Delta x^2}+\frac{1}{\Delta z^2}}}, \frac{1}{c_m\sqrt{2}\sqrt{\frac{1}{\Delta x^2}+\frac{1}{\Delta y^2}}} \right\} \quad (4b)$$

where $i \in \{1, 2, \ldots, n_x\},\ j \in \{1, 2, \ldots, n_y\},\ k \in \{1, 2, \ldots, n_z\}.$ $\square$

A function $f(x)$ is positive definite when $x \neq 0$ implies $f(x) > 0$, and $f(x) = 0$ when $x = 0$ [13]. Note that x can be a vector or a scalar. The proofs for Lemma 2.1 and Lemma 2.2 are shown in Appendix A. In this context stability implies the FDTD algorithm for the 3D model is both numerically and dynamically stable. This means that if we were to reduce Δt to zero or increase the time-step n to infinity, the solution for E and H field components would always remain bounded.

Definition 2.1 – Stability of FDTD algorithm

Suppose we construct a vector $\overline{X}^n$ whose elements consist of all

E and H field components of the model:

$$\overline{X}^n = \begin{bmatrix} E^n_{x(1,1,1)} \\ E^n_{x(2,1,1)} \\ \vdots \\ E^n_{z(n_x+1,n_y+1,n_z)} \\ H^{n-\frac{1}{2}}_{x(1,1,1)} \\ H^{n-\frac{1}{2}}_{x(2,1,1)} \\ \vdots \\ H^{n-\frac{1}{2}}_{z(n_x,n_y,n_z+1)} \end{bmatrix} \tag{5a}$$

$$\dim \overline{X}^n = M = 6n_xn_yn_z + 3(n_xn_y + n_xn_z + n_yn_z) + n_x + n_y + n_z \tag{5b}$$

Then the FDTD algorithm is stable when

$$\left\|\overline{X}^n\right\| \leq C(T) \quad n = 1, 2, 3, \ldots, N \quad \text{and} \quad N = \frac{T}{\Delta t} \qquad \square \tag{5c}$$

The symbol $\|\overline{x}\|$ means taking the 'norm' of a vector $\overline{x}$ [16], which is a measure of the 'distance' between $\overline{x}$ and the origin. $C(T)$ is a positive real value which depends only on T, the maximum computation time. $N = T/\Delta t$ is the maximum sequence. As $\Delta t \to 0$, N will approach infinity. However (5c) dictates that $C(T)$ must be finite as N approaches infinity as long as T is bounded. We allow C to be a function of T as certain solution of the FDTD can increase with time. For instance when there is a source in the model that increases with time, it is then reasonable to expect the field components to gradually increase too. What (5c) means is that the solution remains bounded for finite time interval. If (5c) is not fulfilled as n increases, then the algorithm is not stable. Finally we define the stability theorem:

Theorem 2.3 – Stability theorem for 3D FDTD model

Consider a 3D FDTD model with PEC boundaries of Figure 1, if the model fulfills all the conditions in Lemma 2.2, then a sufficient condition for it to be stable is $P_d \leq 0$. $\square$

The proof is given in Appendix B. The next section will shows how Lemma 2.2 and Theorem 2.3 can be used to determine the stability of a general 3D FDTD model for microwave circuits.

3. APPLICATION EXAMPLE — ESTABLISHING THE STABILITY OF A SOURCELESS 3D PRINTED CIRCUIT BOARD (PCB) MODEL

Assume a PCB model of Figure 1. The PCB model contains non-homogeneous dielectric, lumped resistors, lumped capacitors and nonlinear components such as PN junctions and bipolar junction transistors (BJTs). The FDTD update equations for E and H fields of all these elements can be found in [2–5]. Initially we will consider a sourceless 3D FDTD model for reasons to be explained in Section 4. This means the model will not contain any source, such as the lumped resistive voltage source [2]. We begin by computing the elemental dissipation $\frac{1}{2}(E^{n+1}_{r(i,j,k)} + E^{n}_{r(i,j,k)})J^{n+\frac{1}{2}}_{r(i,j,k)}$ of each element, and show that this is always greater or equal to 0 under normal E and H field values. Furthermore we will also show that $\varepsilon_{r(i,j,k)}$ is always positive under normal field values. Element meeting these two characteristics is called proper. An elemental dissipation > 0 means that the element is absorbing numerical energy from the model. When all the elements are proper, the total dissipation P_d will be equal to 0 or negative, the condition of Theorem 2.3 will be fulfilled. We then limit the time discretization Δt as dictated by (4b) of Lemma 2.2. With the final condition met, Theorem 2.3 tells us that the model will be stable. For simplicity we assume the elements to be oriented in the $+z$ direction. This can always be generalized to elements oriented along other directions.

Lossless Linear Dielectric

For the E_z field of a lossless linear dielectric [3]:

$$E^{n+1}_{z(i,j,k)} = E^{n}_{z(i,j,k)} + \frac{\Delta t}{\varepsilon_r \varepsilon_o} \nabla \times H^{n+\frac{1}{2}}_{z(i,j,k)} \tag{6a}$$

Comparing (6a) with the Canonical FDTD Form for E_z component:

$$J^{n+\frac{1}{2}}_{z(i,j,k)} = 0 \qquad \text{and} \qquad \varepsilon_{z(i,j,k)} = \varepsilon_r \varepsilon_o \tag{6b}$$

Thus elemental dissipation $\frac{1}{2}(E^{n+1}_{z(i,j,k)} + E^{n}_{z(i,j,k)})J^{n+\frac{1}{2}}_{z(i,j,k)} = 0$. Since $\varepsilon_{z(i,j,k)} = \varepsilon_r \varepsilon_o > 0$, the lossless linear dielectric formulation is proper.

Perfect Electric Conductor (PEC)

The electric field in a PEC is always 0. It can be written as:

$$E^{n+1}_{z(i,j,k)} = 0 = E^{n}_{z(i,j,k)} + \frac{\Delta t}{\varepsilon_{PEC}} \nabla \times H^{n+\frac{1}{2}}_{z(i,j,k)} \tag{7}$$

where $\varepsilon_{PEC} \to +\infty$, assuming $E^{0}_{z(i,j,k)} = 0$. Again comparison with Canonical FDTD Form shows that $J^{n+\frac{1}{2}}_{z(i,j,k)} = 0$, implying elemental dissipation is 0. The PEC formulation is proper.

Capacitor

For a lumped capacitor C oriented in z axis, according to [2]:

$$\begin{aligned} E^{n+1}_{z(i,j,k)} &= E^{n}_{z(i,j,k)} + \left(\frac{\dfrac{\Delta t}{\varepsilon_o}}{1 + \dfrac{C\Delta z}{\varepsilon_o \Delta x \Delta y}} \right) \nabla \times H^{n+\frac{1}{2}}_{z(i,j,k)} \\ &= E^{n}_{z(i,j,k)} + \frac{\Delta t}{\varepsilon_o \left(1 + \dfrac{C\Delta z}{\varepsilon_o \Delta x \Delta y} \right)} \nabla \times H^{n+\frac{1}{2}}_{z(i,j,k)} \end{aligned} \tag{8a}$$

Comparing (8a) with Canonical FDTD Form:

$$J^{n+\frac{1}{2}}_{z(i,j,k)} = 0 \quad \text{and} \quad \varepsilon_{z(i,j,k)} = \varepsilon_o \left(1 + \frac{C\Delta z}{\varepsilon_o \Delta x \Delta y} \right) \tag{8b}$$

From (8b) the effective permittivity is always positive and the elemental dissipation is 0. The capacitor formulation is therefore proper.

Linear Dielectric with Loss

For the E_z field of a linear dielectric with conductivity σ, according to [3]:

$$\begin{aligned} E^{n+1}_{z(i,j,k)} &= \left(\frac{1 - \dfrac{\sigma \Delta t}{2\varepsilon}}{1 + \dfrac{\sigma \Delta t}{2\varepsilon}} \right) E^{n}_{z(i,j,k)} + \left(\frac{\dfrac{\Delta t}{\varepsilon}}{1 + \dfrac{\sigma \Delta t}{2\varepsilon}} \right) \nabla \times H^{n+\frac{1}{2}}_{z(i,j,k)} \\ &= E^{n}_{z(i,j,k)} + \frac{\Delta t}{\varepsilon \left(1 + \dfrac{\sigma \Delta t}{2\varepsilon} \right)} \nabla \times H^{n+\frac{1}{2}}_{z(i,j,k)} - 2 \left(\frac{\dfrac{\sigma \Delta t}{2\varepsilon}}{1 + \dfrac{\sigma \Delta t}{2\varepsilon}} \right) E^{n}_{z(i,j,k)} \end{aligned} \tag{9a}$$

Comparing (9a) with Canonical FDTD Form:

$$\varepsilon_{z(i,j,k)} = \varepsilon\left(1 + \frac{\sigma\Delta t}{2\varepsilon}\right) \tag{9b}$$

$$\frac{\Delta t}{\varepsilon\left(1 + \dfrac{\sigma\Delta t}{2\varepsilon_o}\right)} J^{n+\frac{1}{2}}_{z(i,j,k)} = 2\left(\frac{\dfrac{\sigma\Delta t}{2\varepsilon}}{1 + \dfrac{\sigma\Delta t}{2\varepsilon}}\right) \Rightarrow J^{n+\frac{1}{2}}_{z(i,j,k)} = \sigma E^{n}_{z(i,j,k)} \tag{9c}$$

From (9b), $\varepsilon_{z(i,j,k)}$ is always positive, but not the elemental dissipation. Using $x = E^n_{z(i,j,k)}$, $d = \frac{\sigma\Delta t}{2\varepsilon}$ and $y = \nabla \times H^{n+\frac{1}{2}}_{z(i,j,k)}$, the elemental dissipation is:

$$\begin{aligned}\frac{1}{2}\left(E^{n+1}_{z(i,j,k)} + E^{n}_{z(i,j,k)}\right) J^{n+\frac{1}{2}}_{z(i,j,k)} &= \frac{1}{2}\left[\frac{1-d}{1+d}x + \frac{\Delta t}{\varepsilon(1+d)}y + x\right](\sigma x) \\ &= \frac{\sigma}{2(1+d)}\left(2x + \frac{\Delta t}{\varepsilon}y\right)x \end{aligned} \tag{10}$$

This expression is not positive definite, certain combinations of x and y will cause it to become negative. To ensure that it is always positive or 0, we need to introduce extra conditions. Requiring that $\frac{\sigma}{2(1+d)}(2x + \frac{\Delta t}{\varepsilon}y)x \geq 0$:

$$\text{For } x \geq 0: \qquad y \geq -\frac{2\varepsilon}{\Delta t}x \Rightarrow \nabla \times H^{n+\frac{1}{2}}_{z(i,j,k)} \geq -2\frac{\varepsilon}{\Delta t}E^{n}_{z(i,j,k)} \tag{11a}$$

$$\text{For } x < 0: \qquad y < -\frac{2\varepsilon}{\Delta t}x \Rightarrow \nabla \times H^{n+\frac{1}{2}}_{z(i,j,k)} < -2\frac{\varepsilon}{\Delta t}E^{n}_{z(i,j,k)} \tag{11b}$$

Most of the time the conditions of (11a) or (11b) are met, especially when σ is small (low loss at $\sigma < 10$). Extensive real-time examinations of elemental dissipation during FDTD simulation show that the value is always positive for low to medium loss. We do not have to explicitly impose conditions (11a) and (11b) during simulation. Equations (11a) and (11b) imply that current flowing through the element is always limited. This is similar to an electrical circuit with a few paths having low resistance. Even though the low resistance path can support large current, the circuit configuration will tend to limit the current through the paths, ensuring positive power dissipation. In the case of FDTD simulation, the system model will usually limit the magnetic field components surrounding the electric field so that power dissipation is positive. However since finite-difference is only

an approximation to the actual Maxwell's equations, it is expected that the elemental dissipation can become negative once in a while. Extensive simulations show that when σ is substantially greater than 10, the elemental dissipation of (10) results in negative values once in a while. Most lossy dielectric material will have σ much smaller than 1. When the elemental dissipation is negative, we could impose the following equality (complying with (11a) and (11b)) to force it to 0:

$$\nabla \times H^{n+\frac{1}{2}}_{z(i,j,k)} = -2\frac{\varepsilon}{\Delta t} E^{n}_{z(i,j,k)} \tag{12a}$$

Applying (12a) to the update equation of (9a) would result in:

$$E^{n+1}_{z(i,j,k)} = -E^{n}_{z(i,j,k)} \tag{12b}$$

It is found that using (12b) for the case when elemental dissipation is negative does not cause any noticeable change in the FDTD simulation results. A typical flow of updating the E field for lossy dielectric with elemental dissipation checking and correction is shown in Figure 3. Therefore by modifying the update routine for linear dielectric with loss according to the flow of Figure 3, we could again conclude that the formulation is proper. A similar procedure can be used to show that exponential time-stepping scheme [3] for high loss material is also proper, the details are omitted due to lack of space. Formulation such as this where we limit $\nabla \times H^{n+\frac{1}{2}}_{z(i,j,k)}$ given $E^{n}_{z(i,j,k)}$ will be known as conditionally proper.

Resistor

The update equation for a lumped resistive element of resistance R is very similar to the form for linear dielectric with loss. We just replace the term σ with $\frac{\Delta z}{R\Delta x\Delta y}$ [2].

$$E^{n+1}_{z(i,j,k)} = \left(\frac{1-\dfrac{\Delta t\Delta z}{2\varepsilon_o R\Delta x\Delta y}}{1+\dfrac{\Delta t\Delta z}{2\varepsilon_o R\Delta x\Delta y}}\right) E^{n}_{z(i,j,k)} + \left(\frac{\dfrac{\Delta t}{\varepsilon_o}}{1+\dfrac{\Delta t\Delta z}{2\varepsilon_o R\Delta x\Delta y}}\right) \nabla \times H^{n+\frac{1}{2}}_{z(i,j,k)} \tag{13}$$

Using similar modified update routine as in Figure 3, the formulation for resistor is also proper. Again simulation evidence shows that this is not required most of the time, except for low resistance.

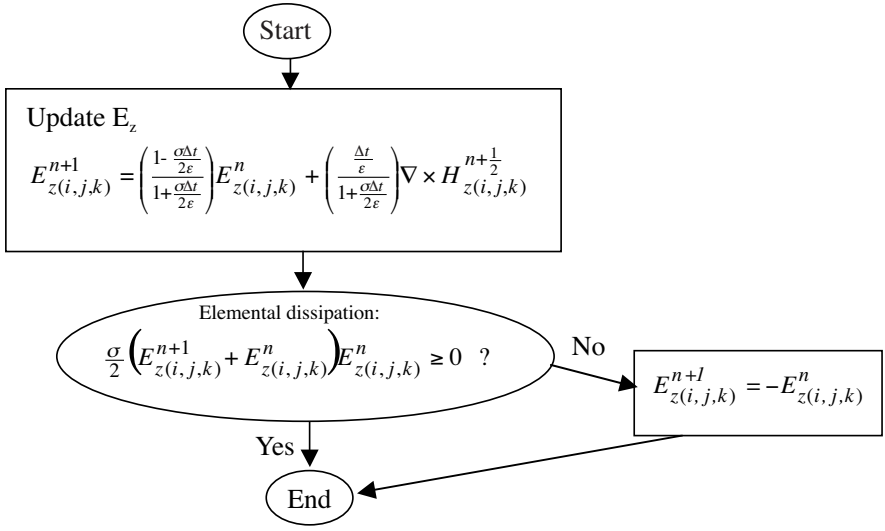

Figure 3. Modified update routine for linear dielectric with nonzero conductivity.

Diode or PN Junction

Consider a PN junction in parallel to the z-axis, with the update equation for the corresponding electric field given by (using the first order approximation) [4]:

$$E^{n+1}_{z(i,j,k)} = E^{n}_{z(i,j,k)} - \frac{C_1}{B_1} \tag{14}$$

$$\begin{aligned} C_1 &= \frac{N\Delta t}{\varepsilon \Delta x \Delta y} I^n_D - \frac{\Delta t}{\varepsilon_o} \nabla \times H^{n+\frac{1}{2}}_{z(i,j,k)}, \\ B_1 &= \frac{\Delta t \Delta z}{\varepsilon \Delta x \Delta y} \left(\frac{1}{2} \frac{dI_D}{dV}(V^n) + \frac{1}{\Delta t} C^n \right) + 1 \end{aligned}$$

$$I^n_D = I_s \left(\exp\left(\frac{V^n}{\eta V_T} \right) - 1 \right), \quad V^n = N E^n_{z(i,j,k)} \Delta z, \quad V_T = \frac{kT}{q}$$

N is the orientation constant, it is $+1$ if the element is oriented in $+z$ direction (i.e., positive current flows in $+z$ direction) [4]. Let $C_2 = \frac{N\Delta t}{\varepsilon_o \Delta x \Delta y} I^n_D$, we could write (14) as:

$$E^{n+1}_{z(i,j,k)} = E^{n}_{z(i,j,k)} + \frac{\Delta t}{\varepsilon_o B_1} \nabla \times H^{n+\frac{1}{2}}_{z(i,j,k)} - \frac{C_2}{B_1}$$

Comparing this with the Canonical FDTD Form:

$$\varepsilon_{z(i,j,k)} = \varepsilon_o B_1 = \frac{\Delta t \Delta z}{\Delta x \Delta y}\left(\frac{1}{2}\frac{dI_D^n}{dV} + \frac{1}{\Delta t}C^n\right) + \varepsilon_o$$

$$\Rightarrow \varepsilon_{z(i,j,k)}\left(E^n_{z(i,j,k)}\right)$$
$$= \frac{\Delta t \Delta z}{\Delta x \Delta y}\left(\frac{I_s}{2\eta V_T}\exp\left(\frac{N E^n_{z(i,j,k)}\Delta z}{\eta V_T}\right) + \frac{1}{\Delta t}C^n\right) + \varepsilon_o \quad (15a)$$

$$\frac{\Delta t}{\varepsilon_o B_1} J^{n+\frac{1}{2}}_{z(i,j,k)} = \frac{C_2}{B_1} \Rightarrow J^{n+\frac{1}{2}}_{z(i,j,k)} = \frac{\varepsilon_o}{\Delta t} C_2 \quad (15b)$$

From (15a) the effective permittivity $\varepsilon_{z(i,j,k)}$ is a function of $E^n_{z(i,j,k)}$ and it is always positive, since C^n (the junction capacitance) and the exponential term always gives positive values. Let us form the following product to examine the sign of elemental dissipation:

$$D = \frac{1}{2}\left(E^{n+1}_{z(i,j,k)} + E^n_{z(i,j,k)}\right) J^{n+\frac{1}{2}}_{z(i,j,k)} = \frac{\varepsilon_o}{2\Delta t}\left(2E^n_{z(i,j,k)} - \frac{C_1}{B_1}\right) C_2 \quad (16)$$

D is a function of $E^n_{z(i,j,k)}$ and $\nabla \times H^{n+\frac{1}{2}}_{z(i,j,k)}$. Using $x = E^n_{z(i,j,k)}$ and $y = \nabla \times H^{n+\frac{1}{2}}_{z(i,j,k)}$, a plot of $D(x, y)$ versus x and y for a typical surface-mount Schottky diode HSMS-2820 [15] is shown in Figure 4. The diode is oriented in $-z$ direction ($N = -1$) and the range of x and y are:

$$x \in [-1000, 7500], \qquad y \in [-5000, 5000]$$

Using $V = N E^n_{z(i,j,k)} \Delta z$, the range for x corresponds to 0.55 to -4.125 Volts, from hard forward biased to hard reverse biased. This range of x and y is typically encountered in simulation for low voltage RF circuits. We could enlarge the coverage if we wish, with similar result obtained. It is seen from Figure 4 that D is weakly influenced by y. Figure 4 confirms that the elemental dissipation is always positive or 0 for normal values of E field. In general it can be shown that this is also true for all practical diode models. Thus from the above arguments, the diode or PN junction formulation is also proper.

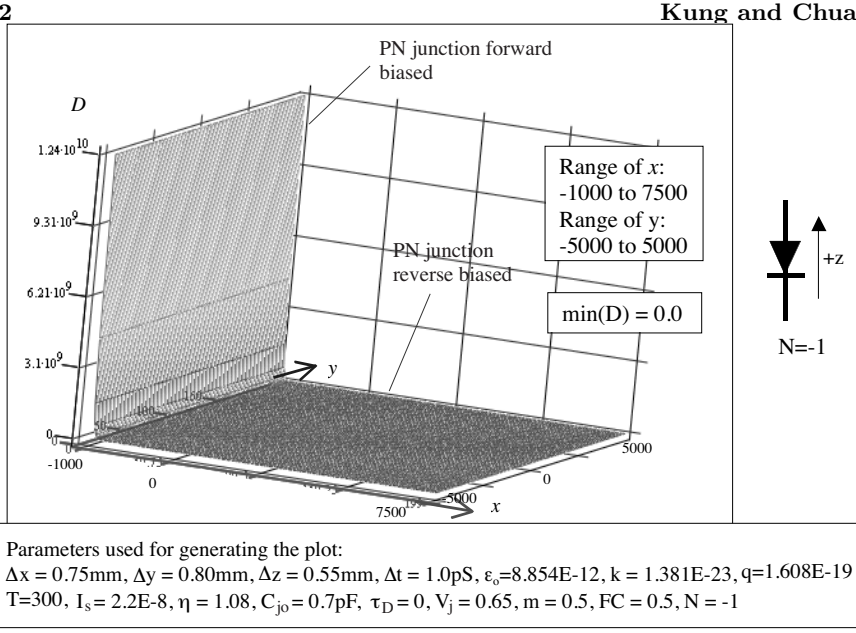

Parameters used for generating the plot:
$\Delta x = 0.75$mm, $\Delta y = 0.80$mm, $\Delta z = 0.55$mm, $\Delta t = 1.0$pS, ε_o=8.854E-12, k = 1.381E-23, q=1.608E-19
T=300, I_S= 2.2E-8, $\eta = 1.08$, C_{jo}= 0.7pF, $\tau_D = 0$, $V_j = 0.65$, m = 0.5, FC = 0.5, N = -1

Figure 4. D versus $x = E^n_{z(i,j,k)}$ and $y = \nabla \times H^{n+\frac{1}{2}}_{z(i,j,k)}$.

Bipolar Junction Transistor (BJT)

A procedure similar to analyzing the characteristics of the PN junction can be employed to analyze the BJT. The BJT is formulated according to [5] where it consists of two PN junctions, the emitter (BE) and the collector (BC) junctions. The elemental dissipation of BE and BC junctions are summed up simultaneously to give the total elemental dissipation of the device. The individual dissipation can be negative, but the total elemental dissipation is always positive or 0 as long as the transistor is suitably biased. We can show that when the BJT is not pushed to extreme saturation or cut-off, the BJT formulation of [5] is also conditionally proper. This is done by verifying the total device dissipation, $\varepsilon_{z(i_c,j_c,k_c)}$ and $\varepsilon_{z(i_e,j_e,k_e)}$ (effective permittivity of BC, BE junctions) are positive definite within the 4 operating regions of a BJT, i.e., active, saturation, inverse and cut-off regions. The BJT formulation is thus conditionally proper. Due to limited space the details will be left out here.

Now suppose the model consists of many cubes of similar size, with $\Delta x = 0.75\,\text{mm},\ \Delta y = 0.8\,\text{mm},\ \Delta z = 0.52\,\text{mm}$. The model is non-magnetic, but the dielectric constant is not uniform, with variation of ε across the model and a portion of the model is free space. Also from

(6b), (8b), (9b) and (15a), the effective permittivity $\varepsilon_{r(i,j,k)}$ is always greater than ε_o. From this information, we conclude that the smallest permittivity equals to ε_o as any dielectric which is not air will have ε_r greater than unity. Using condition (4b) of Lemma 2.2:

$$c_m = \frac{1}{\sqrt{\mu_o \varepsilon_o}} \cong \frac{1}{\sqrt{(4\pi \times 10^{-7})(8.854 \times 10^{-12})}} \cong 2.99796 \times 10^8$$

$$\Delta t < \min \left\{ \begin{array}{l} \left(c_m \sqrt{2} \sqrt{\frac{1}{\Delta y^2} + \frac{1}{\Delta z^2}} \right)^{-1} = 1.02835 \times 10^{-12}, \\ \left(c_m \sqrt{2} \sqrt{\frac{1}{\Delta x^2} + \frac{1}{\Delta z^2}} \right)^{-1} = 1.0079 \times 10^{-12}, \\ \left(c_m \sqrt{2} \sqrt{\frac{1}{\Delta x^2} + \frac{1}{\Delta y^2}} \right)^{-1} = 1.2905 \times 10^{-12} \end{array} \right\}$$

$$\Rightarrow \Delta t < 1.0079 \times 10^{-12}$$

Compare this with CFL Criteria:

$$\Delta t < \frac{1}{c_m \sqrt{\frac{1}{\Delta x^2} + \frac{1}{\Delta y^2} + \frac{1}{\Delta z^2}}} = 1.2573 \times 10^{-12}$$

The new stability criterion has an increase in restriction by 19.84%. Finally we conclude that if all elements used have update equations of the above and $\Delta t < 1.0079 \times 10^{-12}$, then according to Lemma 2.2 and Theorem 2.3, the model of Figure 1 will be stable. This means that if the initial E and H field components at time-step $n = 0$ is not 0, all field components will remain bounded as we advance the time-step n.

Notice that throughout this section we only require the effective permittivity $\varepsilon_{r(i,j,k)}$ of each E field component be positive. Thus the permittivity can change with location, be a nonlinear function of field components and yet the sourceless 3D model is still stable. So the method proposed here could also be used to prove the stability of model with non-homogeneous dielectric and nonlinear dielectric. In the next section, the case when there is a resistive voltage source in the model will be considered.

4. EXTENSION OF THE STABILITY THEOREM TO 3D MODEL WITH SOURCE

Suppose in addition to the elements mentioned in Section 3, the 3D model of Figure 1 also contains a lumped resistive voltage source, with update equation for E_z field given by [2]:

$$\begin{aligned} E^{n+1}_{z(i,j,k)} &= \left(\frac{1-D_z}{1+D_z}\right) E^n_{z(i,j,k)} + \frac{\Delta t}{\varepsilon(1+D_z)} \nabla \times H^{n+\frac{1}{2}}_{z(i,j,k)} \\ &\quad - \left[\frac{2D_z}{(1+D_z)\Delta z}\right] V\left(n+\frac{1}{2}\right) \end{aligned} \tag{17}$$

Where $D_z = \frac{\Delta t \Delta z}{2R_s \varepsilon \Delta x \Delta y}$, $V(n+\frac{1}{2})$ is the independent voltage source as a function of time-step n and R_s being the source resistance. $V(n+\frac{1}{2})$ can represent a constant d.c. source, a pulse, sinusoidal function and so forth. Converting (17) into the Canonical FDTD Form, we observe that the equivalent current density is:

$$J^{n+\frac{1}{2}}_{z(i,j,k)} = \frac{\Delta z}{R_s \Delta x \Delta y}\left(E^n_{z(i,j,k)} + \frac{V(n)}{\Delta z}\right) \tag{18}$$

By introducing $x = E^n_{z(i,j,k)}$, $y = \nabla \times H^{n+\frac{1}{2}}_{z(i,j,k)}$ and $v = \frac{V(n+\frac{1}{2})}{\Delta z}$, the elemental dissipation can be written as:

$$\begin{aligned} D^{n+\frac{1}{2}}(x,y,v) &= \frac{1}{2}\left(E^{n+1}_{z(i,j,k)} + E^n_{z(i,j,k)}\right) J^{n+\frac{1}{2}}_{z(i,j,k)} \\ &= \frac{\Delta z}{2R_s \Delta x \Delta y} \cdot \frac{1}{1+D_z}\left[2x + \frac{\Delta t}{\varepsilon} y\right] x \\ &\quad - \frac{\Delta z}{2R_s \Delta x \Delta y} \cdot \frac{1}{1+D_z}\left[2D_z v - \frac{\Delta t}{\varepsilon} y - 2(1-D_z)x\right] v \end{aligned} \tag{19}$$

Again this equation is indefinite, $D^{n+\frac{1}{2}}$ can be positive or negative. When source element such as (17) is present, P_d can become positive and from Lemma 2.1 the numerical energy V^n of the model can increase with time-step. Assuming v is a constant positive value (we can consider it to be a d.c. voltage source), a plot of the region **A** in the x-y plane where elemental dissipation $D^{n+\frac{1}{2}}$ becomes negative is shown in Figure 5. A similar but inverted region can be easily plotted when v is a constant negative value.

A pertinent question is whether there is any further constraint apart from region **A**? In fact there is. The first constraint is the

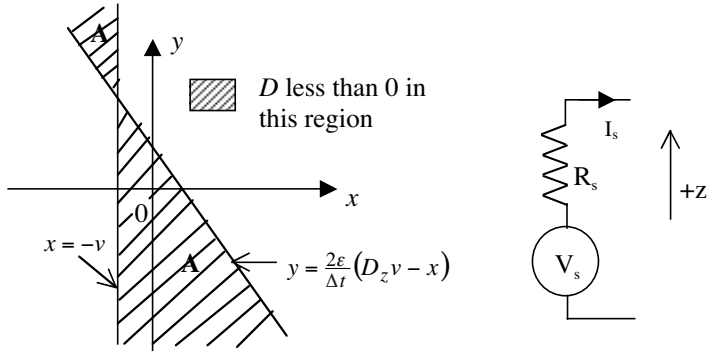

Figure 5. Negative region **A** of the resistive voltage source when $v > 0$ and is constant.

current I_s (see Figure 5) must not be more that V_s/R_s, which represents the source current when the terminals are shorted. There are cases when source current can exceed this limit but for a properly designed circuit V_s/R_s is usually the threshold. The second constraint is for the source of (17) to continuously supply power to the model, elemental dissipation must always be negative or 0 at all sequence n. This means if the (x, y) of sequence n result in $D^{n+\frac{1}{2}} \leq 0$, then (x, y) of sequence $n + 1$ must also result in $D^{n+\frac{3}{2}} \leq 0$. From Appendix C, we can show that these requirements can be expressed mathematically as:

$$y < \frac{2\varepsilon}{\Delta t}(D_z v - x) \tag{20a}$$

$$D^{n+\frac{1}{2}}(x, y, v) \leq 0 \tag{20b}$$

$$x^{n+1} = \left(\frac{1 - D_z}{1 + D_z}\right) x^n + \frac{\Delta t}{\varepsilon(1 + D_z)} y^{n+\frac{1}{2}} - \frac{2D_z}{1 + D_z} v \geq -v \tag{20c}$$

Using the criteria of (20a)–(20c), and assuming $V(n + \frac{1}{2}) = 1$, a new negative region, called **B** is shown in Figure 6a for $D_z < 1$ and Figure 6b for $D_z > 1$. When (x, y) is outside the shaded region B, the resistive voltage source will bound to stop supplying numerical power to the model in future sequence and the E and H field components will start to decrease.

The negative regions **B** identified in Figure 6a and Figure 6b are still quite conservative, nevertheless it is sufficient for our next argument. In order to have $D^{n+\frac{1}{2}} \leq 0$ for all n, the actual region could be smaller than shown. For a resistive voltage source to continuously supply numerical energy to the model, its state (x, y) must always be

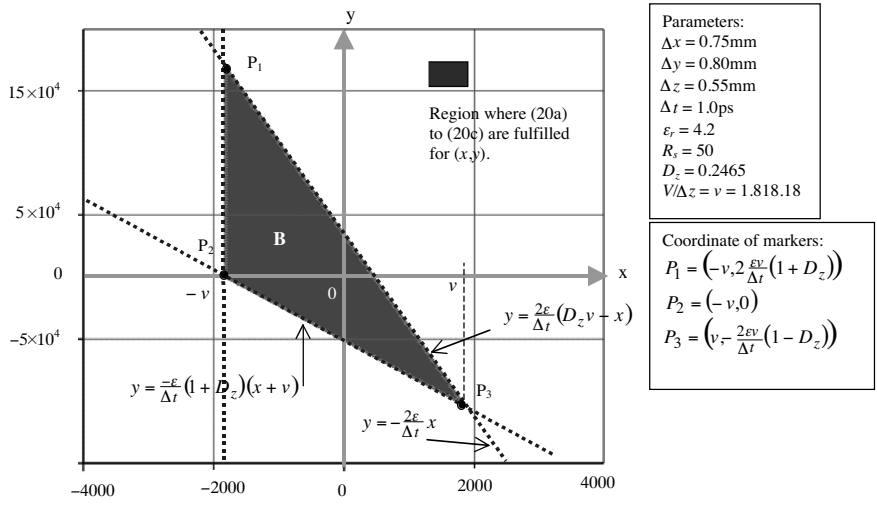

Figure 6a. Negative region for resistive voltage source fulfilling (20a) to (20c), $D_z < 1$. P_1 to P_3 are marker points.

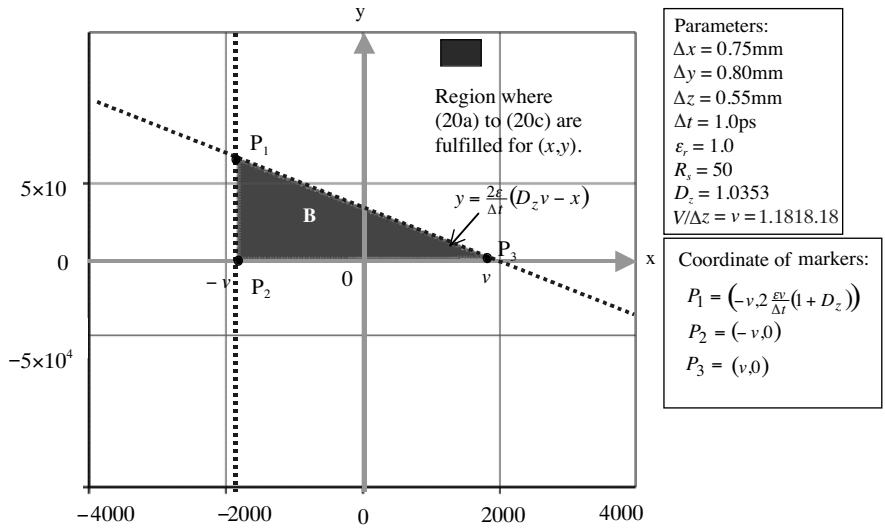

Figure 6b. Negative region for resistive voltage source fulfilling (20a) to (20c), $D_z > 1$.

confined to **B**. Furthermore if the source $V(n+\frac{1}{2})$ is not constant, then we can construct the negative region based on the largest magnitude of $V(n+\frac{1}{2})$. Negative regions for resistive voltage source when $V(n+\frac{1}{2})$ is negative can be constructed in a similar manner using (20a)–(20c). The importance of the negative regions can be summed up as follows. Suppose an FDTD model as in Figure 1 contains all proper or conditionally proper formulations and a few resistive voltage sources. Then initially the numerical energy V^n of the system will increase. Since in Appendix B we have proven that V^n is radially unbounded to all field components, a diverging V^n will entails at least one or more E or H field components that are increasing. Due to the propagating nature of Maxwell's equations, a field component that is increasing without limit will subsequently cause the rest of the model's E and H field components to increase too. The important feature of the negative regions is that it is bounded as long as the source voltage V_s is bounded and R_s greater than 0. If the increment of V^n is not limited by other dissipative elements in the model, (x, y) will eventually cross the boundary of the negative region. Then the elemental dissipation of the resistive voltage source will bound to become positive again and the increment of numerical energy halts. Thus there is a built-in mechanism (due to R_s) in the resistive voltage source formulation to prevent uncontrolled increment of the field components. With this we can conclude that the general FDTD model with resistive voltage sources will be numerically stable if and only if the following 3 conditions are met:

1. Theorem 2.3 is fulfilled.
2. There is no other source except resistive voltage sources.
3. FDTD formulations of other elements are proper or conditionally proper.

5. SIMULATION EXAMPLE

A simulation is carried out to verify the concepts discussed. Here a short conducting trace energized by a resistive voltage source is connected to a parallel RC load. The PEC boundary is used in this experiment. The schematic and the top view of the FDTD model is shown in Figure 7. The simulated voltage across the resistive voltage source and the load is shown in Figure 8(A), while the numerical energy V^n is shown in Figure 8(B). In this model the resistive voltage source is immersed in the dielectric and is z directed. Its voltage function is a single pulse of amplitude 3.3 V, active during 0–2100 ps and then set to 0 beyond 2100 ps. As seen in Figure 8(B) when the voltage

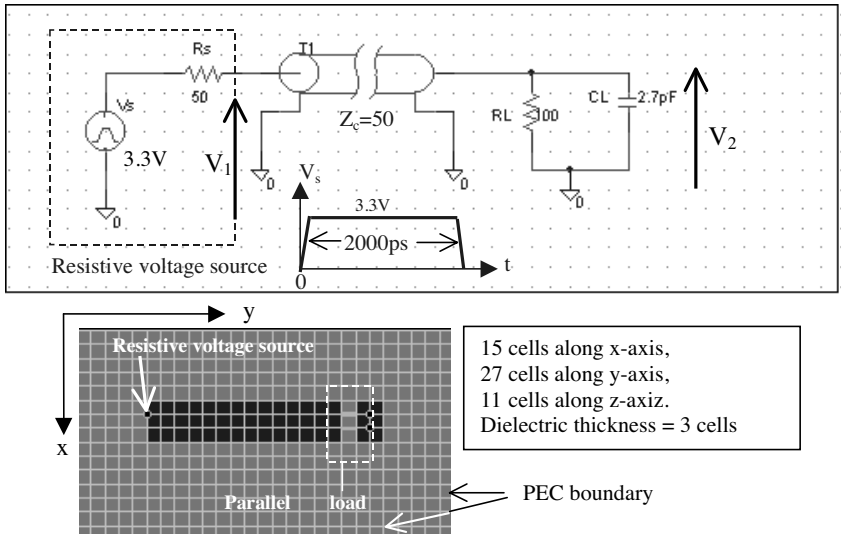

Figure 7. The schematic and top view of the test model.

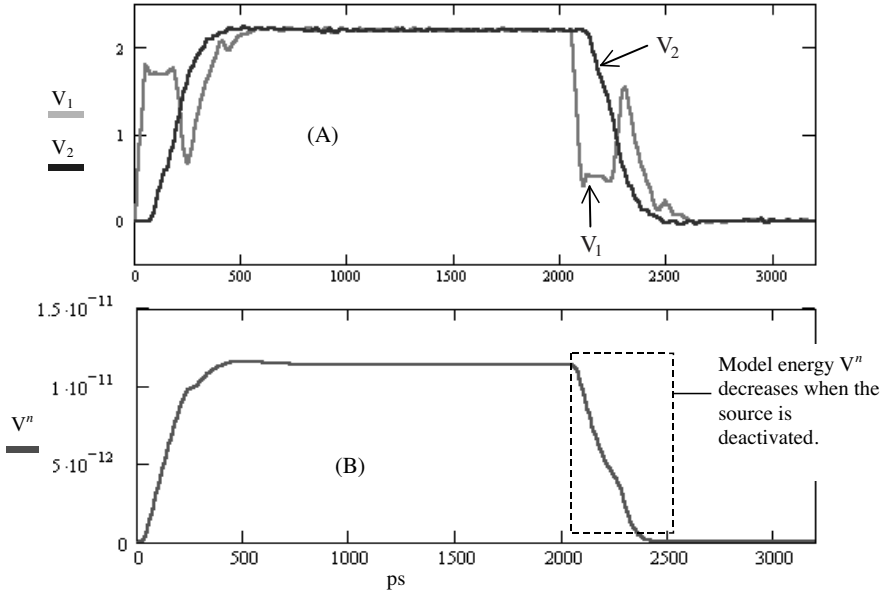

Figure 8. (A) Voltage across the resistive voltage source and the RC load. (B) Numerical energy V^n of the system.

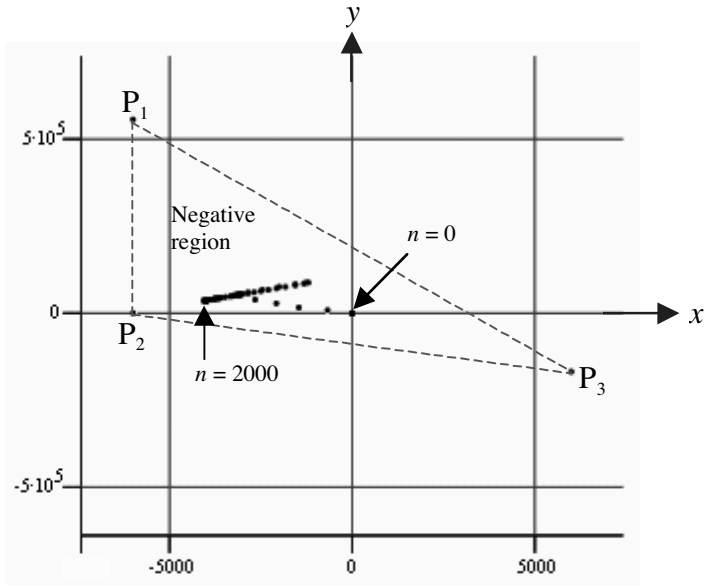

Figure 9. Location of the state (x, y) for $n = 0$ to $n = 2000$ at an interval of 10 time-steps.

source is active, V^n increases rapidly and then saturates, as the 'power' supplied by the source equals the 'power' dissipated by the resistors in the model. During active stage the state (x, y) of the resistive voltage source is determined from the corresponding E and H fields and plotted in the x-y plane of Figure 9. From the result we could clearly see that the coordinate never leaves the negative region. After the voltage V_s is deactivated, the resistive voltage source reverts to a normal resistor model. We observe that the numerical energy V^n of the model starts to decline, as now all the elements in the model are proper.

6. CONCLUSIONS

The theorems in Section 2 are useful. They overcome the limitations of Von-Neumann approach, which result in the CFL Criterion. First and foremost, they can be used to determine and ensure the stability of Yee's FDTD model for microwave circuit or high-speed PCB with the following conditions: (a) Variable and nonlinear dielectric constant. (b) Containing linear and nonlinear lumped elements. (c) Including the effect of PEC boundary. In applying Theorem 2.3, the only requirement for permittivity ε is that it must be positive for all E

field components while the requirement for permeability μ is that it must be equal to μ_o for all H field components.

Secondly, the conditions imposed on $\varepsilon_{r(i,j,k)}$, $J^{n+\frac{1}{2}}_{z(i,j,k)}$ and P_d in Lemma 2.2 and Theorem 2.3 can be used as a test to check whether the FDTD formulation of a lumped element is proper. For a new lumped element, we can write its E field update equation in the Canonical FDTD Form, determine the equivalent current density and compute its elemental dissipation $\frac{1}{2}(E^{n+1}_{z(i,j,k)} + E^{n}_{z(i,j,k)})J^{n+\frac{1}{2}}_{z(i,j,k)}$ against all possible combinations of dependent field components as shown in Section 3. As long as the elemental dissipation is greater or equal to 0 and $\varepsilon_{r(i,j,k)} > 0$, we know that the formulation is proper and will not contribute to instability of the model.

The Von-Neumann and other linear approaches cannot be used to analyze stability of the system under the above conditions of (a)–(c), and traditionally rule-of-thumbs are used to ensure that the FDTD model is stable. In addition, the approach presented here can also be extended to include:

- Variable and nonlinear permeability.
- Non-uniform cell size.
- Dispersive elements and lumped inductors.
- Absorbing boundary condition.

The first and second extension can be carried out by writing $\mu = \mu_{r(i,j,k)}$ and reformulating the condition for V^n to be positive definite. The third extension can be carried out by implement a monitoring algorithm much like Figure 3. The fourth extension can be achieved by introducing a few layers of cells with conductivity before the PEC boundary. A better approach would be to introduce magnetic conductivity and magnetic current. Then formulate an absorbing boundary condition (ABC) based on Perfectly Matched Layer (PML) method [3]. Similar procedures as in the previous sections can be used to derive extended theorem incorporating magnetic loss of $\frac{1}{2}\left(H^{n+\frac{1}{2}}_{r(i,j,k)} + H^{n-\frac{1}{2}}_{r(i,j,k)}\right) M^{n}_{r(i,j,k)}$, where $M^{n}_{r(i,j,k)}$ is the corresponding magnetic current density.

The method does have some disadvantages. It will fail when there is update equations for either E or H field that cannot be written in the Canonical FDTD Form. Also the condition for Δt is slightly more rigid than CFL Criterion. Finally the effect of absorbing boundary condition based on mathematical formulation such as Mur's ABC have not been established. Efforts will be made to include this as well in future research.

APPENDIX A. FINITE-DIFFERENCE POWER RELATION AND V^N

Consider Figure A1, three lump elements coincide with $E_{x(i,j,k)}$, $E_{y(i,j,k)}$ and $E_{z(i,j,k)}$ in Cube (i,j,k). The current density for each element is $J_{x(i,j,k)}$, $J_{y(i,j,k)}$, and $J_{z(i,j,k)}$.

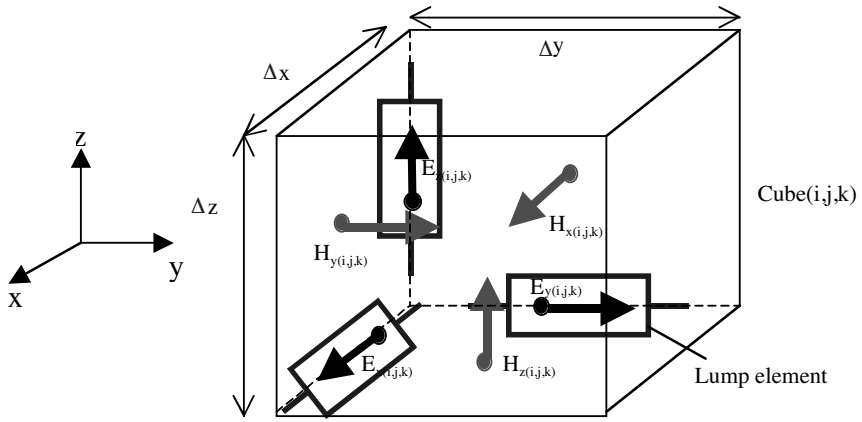

Figure A1. Lump elements coincide with $E_{x(i,j,k)}$, $E_{y(i,j,k)}$ and $E_{z(i,j,k)}$.

The numerical power dissipation density $(\overline{E}\cdot\overline{J})$ at $n+\frac{1}{2}$ time step for Cube (i,j,k) is taken as:

$$\begin{aligned} P^{n+\frac{1}{2}}_{(i,j,k)} &= \sum_{r=x,y,z} \frac{1}{2}\left(E^{n+1}_{r(i,j,k)} + E^{n}_{r(i,j,k)}\right) J^{n+\frac{1}{2}}_{r(i,j,k)} \\ &= (E\cdot J)^{n+\frac{1}{2}}_{x} + (E\cdot J)^{n+\frac{1}{2}}_{y} + (E\cdot J)^{n+\frac{1}{2}}_{z} \end{aligned} \tag{A1}$$

Consider the first term of (A1). Solving (1d) for $J^{n+\frac{1}{2}}_{x(i,j,k)}$:

$$\begin{aligned} (E\cdot J)^{n+\frac{1}{2}}_{x} &= \frac{1}{2}\left(E^{n+1}_{x(i,j,k)} + E^{n}_{x(i,j,k)}\right) \\ &\quad \cdot\left[-\left(E^{n+1}_{x(i,j,k)} - E^{n}_{x(i,j,k)}\right) + \frac{\Delta t}{\varepsilon_{x(i,j,k)}}\nabla\times H^{n+\frac{1}{2}}_{x(i,j,k)}\right]\left(\frac{\varepsilon_{x(i,j,k)}}{\Delta t}\right) \\ &= -\frac{1}{2}\left(\frac{\varepsilon_{x(i,j,k)}}{\Delta t}\right)\left((E^{n+1}_{x(i,j,k)})^2 - (E^{n}_{x(i,j,k)})^2\right) \\ &\quad +\frac{1}{2}\left(E^{n+1}_{x(i,j,k)} + E^{n}_{x(i,j,k)}\right)\left(\nabla\times H^{n+\frac{1}{2}}_{x(i,j,k)}\right) \end{aligned}$$

Now let us introduce three new notations:

$$\left(E^n \cdot \nabla \times H^{n+\frac{1}{2}}\right)_{(i,j,k)} = \sum_{r=x,y,z} E^n_{r(i,j,k)} \nabla \times H^{n+\frac{1}{2}}_{r(i,j,k)} \quad \text{(A2)}$$

$$\left(H^{n+\frac{1}{2}} \cdot \nabla \times E^n\right)_{(i,j,k)} = \sum_{r=x,y,z} H^{n+\frac{1}{2}}_{r(i,j,k)} \nabla \times E^n_{r(i,j,k)} \quad \text{(A3)}$$

$$\nabla \cdot \left(E^{n+1} \times H^{n+\frac{1}{2}}\right)_{(i,j,k)} = -\left(E^{n+1} \cdot \nabla \times H^{n+\frac{1}{2}}\right)_{(i,j,k)} + \left(H^{n+\frac{1}{2}} \cdot \nabla \times E^{n+1}\right)_{(i,j,k)} \quad \text{(A4)}$$

In (A2)–(A4) the time-step is not critical, for instance we could replace n with $n+1$ without affecting the validity. Using (A2) and summing up the x, y and z components, (A1) can be written in a more compact form:

$$-P^{n+\frac{1}{2}}_{(i,j,k)} = \frac{1}{2}\left\{ \begin{array}{l} \displaystyle\sum_{r=x,y,z} \frac{\varepsilon_{r(i,j,k)}}{\Delta t}\left((E^{n+1}_{r(i,j,k)})^2 - (E^n_{r(i,j,k)})^2\right) \\ -\left(E^{n+1} \cdot \nabla \times H^{n+\frac{1}{2}}\right)_{(i,j,k)} - \left(E^n \cdot \nabla \times H^{n+\frac{1}{2}}\right)_{(i,j,k)} \end{array} \right\} \quad \text{(A5)}$$

Adding and subtracting $(H^{n+\frac{1}{2}} \cdot \nabla \times E^{n+1})_{(i,j,k)}$ and $(H^{n+\frac{1}{2}} \cdot \nabla \times E^n)_{(i,j,k)}$ to the second and third terms on the right-hand side of (A5):

$$\left(E^{n+1} \cdot \nabla \times H^{n+\frac{1}{2}}\right)_{(i,j,k)} = \left(H^{n+\frac{1}{2}} \cdot \nabla \times E^{n+1}\right)_{(i,j,k)} - \nabla \cdot \left(E^{n+1} \times H^{n+\frac{1}{2}}\right)_{(i,j,k)} \quad \text{(A6a)}$$

$$\left(E^{n} \cdot \nabla \times H^{n+\frac{1}{2}}\right)_{(i,j,k)} = \left(H^{n+\frac{1}{2}} \cdot \nabla \times E^{n}\right)_{(i,j,k)} - \nabla \cdot \left(E^{n} \times H^{n+\frac{1}{2}}\right)_{(i,j,k)} \quad \text{(A6b)}$$

Using (A3), (1a)–(1c), the first term on the right-hand side of (A6a), (A6b) can be expanded as:

$$\left(H^{n+\frac{1}{2}} \cdot \nabla \times E^{n+1}\right)_{(i,j,k)} = -\sum_{r=x,y,z} \frac{\mu}{\Delta t}\left(-(H^{n+\frac{1}{2}}_{r(i,j,k)})^2 + (H^{n+\frac{1}{2}}_{r(i,j,k)})^2\right) + \left(H^{n+\frac{1}{2}} \cdot \nabla \times E^{n+1}\right)_{(i,j,k)} \quad \text{(A7a)}$$

$$\left(H^{n+\frac{1}{2}} \cdot \nabla \times E^n\right)_{(i,j,k)} = -\sum_{r=x,y,z} \frac{\mu}{\Delta t}\left((H^{n+\frac{1}{2}}_{r(i,j,k)})^2 - (H^{n-\frac{1}{2}}_{r(i,j,k)})^2\right) - \left(H^{n-\frac{1}{2}} \cdot \nabla \times E^n\right)_{(i,j,k)} \quad \text{(A7b)}$$

Finally substituting (A7a), (A7b), (A6a) and (A6b) into (A5), we obtain the desired expression for numerical power dissipation density at Cube (i, j, k):

$$\begin{aligned}
&\frac{1}{2\Delta t}\left[\sum_{r=x,y,z}\left(\varepsilon_{r(i,j,k)}(E^{n+1}_{r(i,j,k)})^2 + \mu(H^{n+\frac{1}{2}}_{r(i,j,k)})^2\right) - \Delta t\left(H^{n+\frac{1}{2}} \cdot \nabla \times E^{n+1}\right)_{(i,j,k)}\right] \\
&-\frac{1}{2\Delta t}\left[\sum_{r=x,y,z}\left(\varepsilon_{r(i,j,k)}(E^{n}_{r(i,j,k)})^2 + \mu(H^{n-\frac{1}{2}}_{r(i,j,k)})^2\right) - \Delta t\left(H^{n-\frac{1}{2}} \cdot \nabla \times E^{n}\right)_{(i,j,k)}\right] \\
&+\frac{1}{2}\left\{\nabla \cdot \left(E^{n+1} \times H^{n+\frac{1}{2}}\right)_{(i,j,k)} + \nabla \cdot \left(E^{n} \times H^{n+\frac{1}{2}}\right)_{(i,j,k)}\right\} \\
&= -P^{n+\frac{1}{2}}_{(i,j,k)} = -\left\{\sum_{r=x,y,z}\frac{1}{2}\left(E^{n+1}_{z(i,j,k)} + E^{n}_{z(i,j,k)}\right) J^{n+\frac{1}{2}}_{r(i,j,k)}\right\} \quad \text{(A8)}
\end{aligned}$$

Equation (A8) only applies to a single Yee's cell at index (i, j, k). Now we determine the form for (A8) when sum up over all the cells. We could expand the expression in the third braces on the left-hand side of (A8) using (A2)–(A4). For E and H field components at n and $n + \frac{1}{2}$ time steps:

$$\begin{aligned}
\nabla \cdot \left(E^n \times H^{n+\frac{1}{2}}\right)_{(i,j,k)} &= \nabla \cdot \left(E^n \times H^{n+\frac{1}{2}}\right)_{(i,j,k)x} + \nabla \cdot \left(E^n \times H^{n+\frac{1}{2}}\right)_{(i,j,k)y} \\
&\quad + \nabla \cdot \left(E^n \times H^{n+\frac{1}{2}}\right)_{(i,j,k)z} \\
&= \frac{1}{\Delta y}\left[E^n_{x(i,j,k)} H^{n+\frac{1}{2}}_{z(i,j-1,k)} - E^n_{x(i,j+1,k)} H^{n+\frac{1}{2}}_{z(i,j,k)}\right] \\
&\quad + \frac{1}{\Delta z}\left[E^n_{x(i,j,k+1)} H^{n+\frac{1}{2}}_{y(i,j,k)} - E^n_{x(i,j,k)} H^{n+\frac{1}{2}}_{y(i,j,k-1)}\right] \\
&\quad + \frac{1}{\Delta z}\left[E^n_{y(i,j,k)} H^{n+\frac{1}{2}}_{x(i,j,k-1)} - E^n_{y(i,j,k+1)} H^{n+\frac{1}{2}}_{x(i,j,k)}\right]
\end{aligned}$$

$$+\frac{1}{\Delta x}\left[E^n_{y(i+1,j,k)}H^{n+\frac{1}{2}}_{z(i,j,k)} - E^n_{y(i,j,k)}H^{n+\frac{1}{2}}_{z(i-1,j,k)}\right]$$
$$+\frac{1}{\Delta x}\left[E^n_{z(i,j,k)}H^{n+\frac{1}{2}}_{y(i-1,j,k)} - E^n_{z(i+1,j,k)}H^{n+\frac{1}{2}}_{y(i,j,k)}\right]$$
$$+\frac{1}{\Delta y}\left[E^n_{z(i,j+1,k)}H^{n+\frac{1}{2}}_{x(i,j,k)} - E^n_{z(i,j,k)}H^{n+\frac{1}{2}}_{x(i,j-1,k)}\right] \tag{A9}$$

The total sum of $\sum_{k=1}^{n_z}\sum_{j=1}^{n_y}\sum_{i=1}^{n_x}\nabla\cdot(E^n\times H^{n+\frac{1}{2}})_{(i,j,k)}$ can be obtained by considering the sum of each component. The details are not difficult but very tedious; it will not be shown due to lack of space. For a 3D model consisting of $(n_x n_y n_z)$ cubes, it can be shown that:

$$\sum_{k=1}^{n_z}\sum_{j=1}^{n_y}\sum_{i=1}^{n_x}\nabla\cdot(E^n\times H^{n+\frac{1}{2}})_{(i,j,k)} =$$
$$\frac{1}{\Delta x}\sum_{k=1}^{n_z}\sum_{j=1}^{n_y}\Bigg(E^n_{y(n_x+1,j,k)}H^{n+\frac{1}{2}}_{z(n_x,j,k)} - E^n_{y(1,j,k)}H^{n+\frac{1}{2}}_{z(0,j,k)}$$
$$- E^n_{z(n_x+1,j,k)}H^{n+\frac{1}{2}}_{y(n_x,j,k)} + E^n_{z(1,j,k)}H^{n+\frac{1}{2}}_{y(0,j,k)}\Bigg)$$
$$+\frac{1}{\Delta y}\sum_{k=1}^{n_z}\sum_{i=1}^{n_x}\Bigg(E^n_{z(i,n_y+1,k)}H^{n+\frac{1}{2}}_{x(i,n_y,k)} - E^n_{z(i,1,k)}H^{n+\frac{1}{2}}_{x(i,0,k)}$$
$$- E^n_{x(i,n_y+1,k)}H^{n+\frac{1}{2}}_{z(i,n_y,k)} + E^n_{x(i,1,k)}H^{n+\frac{1}{2}}_{z(i,0,k)}\Bigg)$$
$$+\frac{1}{\Delta z}\sum_{j=1}^{n_y}\sum_{i=1}^{n_x}\Bigg(E^n_{x(i,j,n_z+1)}H^{n+\frac{1}{2}}_{y(i,j,n_z)} - E^n_{x(i,j,1)}H^{n+\frac{1}{2}}_{y(i,j,0)}$$
$$- E^n_{y(i,j,n_z+1)}H^{n+\frac{1}{2}}_{x(i,j,n_z)} + E^n_{y(i,j,1)}H^{n+\frac{1}{2}}_{x(i,j,0)}\Bigg) \tag{A10}$$

Equation (A10) is also valid when E^n is replaced by E^{n+1}. Finally by summing equation (A8) for all the cubes in a 3D model, we obtain the total numerical power relation:

$$\frac{1}{2}\sum_{k=1}^{n_z}\sum_{j=1}^{n_y}\sum_{i=1}^{n_x}\Bigg[\sum_{r=x,y,z}\left(\varepsilon_{r(i,j,k)}(E^{n+1}_{r(i,j,k)})^2 + \mu(H^{n+\frac{1}{2}}_{r(i,j,k)})^2\right)$$
$$- \Delta t\left(H^{n+\frac{1}{2}}\cdot\nabla\times E^{n+1}\right)_{(i,j,k)}\Bigg]$$

$$
\begin{aligned}
&-\frac{1}{2}\sum_{k=1}^{n_z}\sum_{j=1}^{n_y}\sum_{i=1}^{n_x}\left[\sum_{r=x,y,z}\left(\varepsilon_{r(i,j,k)}(E^n_{r(i,j,k)})^2+\mu(H^{n-\frac{1}{2}}_{r(i,j,k)})^2\right)\right.\\
&\qquad\left.-\Delta t\left(H^{n-\frac{1}{2}}\cdot\nabla\times E^n\right)_{(i,j,k)}\right]\\
&+\frac{\Delta t}{2}\sum_{k=1}^{n_z}\sum_{j=1}^{n_y}\sum_{i=1}^{n_x}\left\{\nabla\cdot\left(E^{n+1}\times H^{n+\frac{1}{2}}\right)_{(i,j,k)}+\nabla\cdot\left(E^n\times H^{n+\frac{1}{2}}\right)_{(i,j,k)}\right\}\\
&=-\Delta t\sum_{k=1}^{n_z}\sum_{j=1}^{n_y}\sum_{i=1}^{n_x}\left\{\sum_{r=x,y,z}\frac{1}{2}\left(E^{n+1}_{r(i,j,k)}+E^n_{r(i,j,k)}\right)J^{n+\frac{1}{2}}_{r(i,j,k)}\right\}
\end{aligned}
\tag{A11}
$$

It is understood that (A10) will be used to expand the third term on the left-hand side of (A11). Equation (A11) is the finite-difference Poynting power relation for a 3D FDTD model with the update equations for E and H fields fulfilling the canonical form of (1a)–(1f). Both (A10) and (A11) are still formidable to apply. It will be applied to a model with PEC boundary surfaces as shown in Figure 1. All the following E field components on the boundaries will be zero regardless of time-step n:

$$
\begin{aligned}
E^n_{x(i,1,k)}, E^n_{x(i,n_y+1,k)}, E^n_{x(i,j,1)}, E^n_{x(i,j,n_z+1)} &= 0\\
E^n_{y(1,j,k)}, E^n_{y(n_x+1,j,k)}, E^n_{y(i,j,1)}, E^n_{y(i,j,n_z+1)} &= 0\\
E^n_{z(1,j,k)}, E^n_{z(n_x+1,j,k)}, E^n_{z(i,1,k)}, E^n_{z(i,n_y+1,k)} &= 0
\end{aligned}
$$

Substituting these components into (A10), we observe that:

$$
\sum_{k=1}^{n_z}\sum_{j=1}^{n_y}\sum_{i=1}^{n_x}\left\{\nabla\cdot\left(E^{n+1}\times H^{n+\frac{1}{2}}\right)_{(i,j,k)}+\nabla\cdot\left(E^n\times H^{n+\frac{1}{2}}\right)_{(i,j,k)}\right\}=0
\tag{A12}
$$

Thus putting (A12) into the numerical power relation (A11) yields:

$$
\begin{aligned}
&\frac{1}{2}\sum_{k=1}^{n_z}\sum_{j=1}^{n_y}\sum_{i=1}^{n_x}\left[\sum_{r=x,y,z}\left(\varepsilon_{r(i,j,k)}(E^{n+1}_{r(i,j,k)})^2+\mu(H^{n+\frac{1}{2}}_{r(i,j,k)})^2\right)\right.\\
&\qquad\left.-\Delta t\left(H^{n+\frac{1}{2}}\cdot\nabla\times E^{n+1}\right)_{(i,j,k)}\right]\\
&-\frac{1}{2}\sum_{k=1}^{n_z}\sum_{j=1}^{n_y}\sum_{i=1}^{n_x}\left[\sum_{r=x,y,z}\left(\varepsilon_{r(i,j,k)}(E^n_{r(i,j,k)})^2+\mu(H^{n-\frac{1}{2}}_{r(i,j,k)})^2\right)\right.
\end{aligned}
$$

$$- \Delta t \left(H^{n-\frac{1}{2}} \cdot \nabla \times E^n \right)_{(i,j,k)} \Bigg]$$

$$= -\Delta t \sum_{k=1}^{n_z} \sum_{j=1}^{n_y} \sum_{i=1}^{n_x} \left\{ \sum_{r=x,y,z} \frac{1}{2} \left(E^{n+1}_{r(i,j,k)} + E^n_{r(i,j,k)} \right) J^{n+\frac{1}{2}}_{r(i,j,k)} \right\} \quad \text{(A13)}$$

We observe that the left-hand side of (A13) consists of two expressions in similar form. The former expression contains E and H field components at time-step $n+1$ and $n+\frac{1}{2}$. The latter expression contains E and H field components at time-step n and $n-\frac{1}{2}$. Multiplying left and right-hand side with ΔV and calling the first expression on the left V^{n+1} and the second expression V^n, (A13) can then be written in a compact form:

$$V^{n+1} - V^n = \Delta t \cdot P_d \quad \text{(A14)}$$

By expanding V^n using the definitions of (A3) and (1g), we see that V^n is similar to the definition in (2a) and P_d is as given in (2b). This proves Lemma 2.1. □

The following steps will derive the positive definite criteria for V^n. Consider the expanded expression for V^n:

$$V^n = \frac{\Delta V}{2} \sum_{k=1}^{n_z} \sum_{j=1}^{n_y} \sum_{i=1}^{n_x} \left[\begin{array}{l} \displaystyle\sum_{r=x,y,z} \left(\varepsilon_{r(i,j,k)} (E^n_{r(i,j,k)})^2 + \mu (H^{n-\frac{1}{2}}_{r(i,j,k)})^2 \right) \\ -H^{n-\frac{1}{2}}_{x(i,j,k)} \left[b_y \left(E^n_{z(i,j+1,k)} - E^n_{z(i,j,k)} \right) \right. \\ \qquad \left. - b_z \left(E^n_{y(i,j,k+1)} - E^n_{y(i,j,k)} \right) \right] \\ -H^{n-\frac{1}{2}}_{y(i,j,k)} \left[b_z \left(E^n_{x(i,j,k+1)} - E^n_{x(i,j,k)} \right) \right. \\ \qquad \left. - b_x \left(E^n_{z(i+1,j,k)} - E^n_{z(i,j,k)} \right) \right] \\ -H^{n-\frac{1}{2}}_{z(i,j,k)} \left[b_x \left(E^n_{y(i+1,j,k)} - E^n_{y(i,j,k)} \right) \right. \\ \qquad \left. - b_y \left(E^n_{x(i,j+1,k)} - E^n_{x(i,j,k)} \right) \right] \end{array} \right] \quad \text{(A15)}$$

Where $b_x = \frac{\Delta t}{\Delta x}$, $b_y = \frac{\Delta t}{\Delta y}$ and $b_z = \frac{\Delta t}{\Delta z}$. We could see that (A15) is a *quadratic form*, with the E and H field components constituting the variables. A quadratic expression can be written in matrix form

[14, 16], for example:

$$\begin{aligned} f(x_1, x_2, x_3) &= 2x_1^2 + x_2^2 + 3x_3^2 + 4x_1x_2 - 6x_1x_3 + 11x_2x_3 \\ &= \begin{bmatrix} x_1 & x_2 & x_3 \end{bmatrix}^T \begin{bmatrix} 2 & 2 & -3 \\ 2 & 1 & \frac{11}{2} \\ -3 & \frac{11}{2} & 3 \end{bmatrix} \begin{bmatrix} x_1 \\ x_2 \\ x_3 \end{bmatrix} \end{aligned}$$

The square matrix is symmetry. When $f(x_1, x_2, x_3)$ is positive definite, $f > 0$ when $x_1, x_2, x_3 \neq 0$ and $f(0, 0, 0) = 0$. To show that $f(x_1, x_2, x_3)$ is positive definite, one can analyze the eigenvalues of the square matrix. Only when all eigenvalues are greater than 0 is $f(x_1, x_2, x_3)$ positive definite. Another approach is to apply Sylvester's Criteria [14]. Sylverster's Criteria states that all the principal minors of the square matrix must be larger than 0 for $f(x_1, x_2, x_3)$ to be positive definite. By examining the principal minors of the matrix:

$$P_1 = |2| = 2,\ P_2 = \begin{vmatrix} 2 & 2 \\ 1 & 1 \end{vmatrix} = -2,\ P_3 = \begin{vmatrix} 2 & 2 & -3 \\ 2 & 1 & 11/2 \\ -3 & 11/2 & 3 \end{vmatrix} = -141.5$$

Not all principal minors are positive, so this quadratic form is not positive definite. Both approaches are extremely difficult to apply directly to equation (A15) due to the large number of variables. The square matrix will be extremely large and computing its eigenvalues or principal minors will require huge computing effort. Furthermore this brute force approach is not practical, as we have to recompute the eigenvalues or principal minors every time we change the configuration of the model.

Therefore we seek an alternative method. We consider breaking the right-hand side of (A15) into groups consisting of a few variables, with each group ideally also of quadratic form. Using Sylvester's Criteria, conditions for each group to be positive definite are derived and by combining the conditions from all group, a general criterion can be obtained. This criterion is general in that if Δx, Δy, Δz, Δt, ε and μ of each cube fulfill the general criteria, the function V^n on the whole will be positive definite. The basis of choosing the group is that we would like the positive definite criteria to hold when there is variation of permittivity (or effective permittivity) $\varepsilon_{(i,j,k)}$ across the model. Suppose we just pay particular attention to 4 cubes, which are adjacent to each other, as shown in Figure A2. For simplicity we assume the model to be non-magnetic $\mu_{(i,j,k)} = \mu = \mu_o$ and all cells to be similar in size. Expanding (A15) and just concentrating on the

stored energy in the 4 cubes of Figure A2.

$$
\begin{aligned}
V^n = \frac{\Delta V}{2}\Bigg\{ & \cdots\cdots + \sum_{r=x,y,z}\left(\varepsilon_{r(i,j,k)}(E^n_{r(i,j,k)})^2 + 4\cdot\frac{1}{4}\mu(H^{n-\frac{1}{2}}_{r(i,j,k)})^2\right) \\
& -H^{n-\frac{1}{2}}_{x(i,j,k)}\left[b_y\left(E^n_{z(i,j+1,k)}-E^n_{z(i,j,k)}\right) - b_z\left(E^n_{y(i,j,k+1)}-E^n_{y(i,j,k)}\right)\right] \\
& -H^{n-\frac{1}{2}}_{y(i,j,k)}\left[b_z\left(E^n_{x(i,j,k+1)}-E^n_{x(i,j,k)}\right) - b_x\left(E^n_{z(i+1,j,k)}-E^n_{z(i,j,k)}\right)\right] \\
& -H^{n-\frac{1}{2}}_{z(i,j,k)}\left[b_x\left(E^n_{y(i+1,j,k)}-E^n_{y(i,j,k)}\right) - b_y\left(E^n_{x(i,j+1,k)}-E^n_{x(i,j,k)}\right)\right] \\
& + \sum_{r=x,y,z}\left(\varepsilon_{r(i-1,j,k)}(E^n_{r(i-1,j,k)})^2 + 4\cdot\frac{1}{4}\mu(H^{n-\frac{1}{2}}_{r(i-1,j,k)})^2\right) \\
& -H^{n-\frac{1}{2}}_{x(i-1,j,k)}\left[b_y\left(E^n_{z(i-1,j+1,k)}-E^n_{z(i-1,j,k)}\right) - b_z\left(E^n_{y(i-1,j,k+1)}-E^n_{y(i-1,j,k)}\right)\right] \\
& -H^{n-\frac{1}{2}}_{y(i-1,j,k)}\left[b_z\left(E^n_{x(i-1,j,k+1)}-E^n_{x(i-1,j,k)}\right) - b_x\left(E^n_{z(i,j,k)}-E^n_{z(i-1,j,k)}\right)\right] \\
& -H^{n-\frac{1}{2}}_{z(i-1,j,k)}\left[b_x\left(E^n_{y(i,j,k)}-E^n_{y(i-1,j,k)}\right) - b_y\left(E^n_{x(i-1,j+1,k)}-E^n_{x(i-1,j,k)}\right)\right] \\
& + \sum_{r=x,y,z}\left(\varepsilon_{r(i,j,k-1)}(E^n_{r(i,j,k-1)})^2 + 4\cdot\frac{1}{4}\mu(H^{n-\frac{1}{2}}_{r(i,j,k-1)})^2\right) \\
& -H^{n-\frac{1}{2}}_{x(i,j,k-1)}\left[b_y\left(E^n_{z(i,j+1,k-1)}-E^n_{z(i,j,k-1)}\right) - b_z\left(E^n_{y(i,j,k)}-E^n_{y(i,j,k-1)}\right)\right] \\
& -H^{n-\frac{1}{2}}_{y(i,j,k-1)}\left[b_z\left(E^n_{x(i,j,k)}-E^n_{x(i,j,k-1)}\right) - b_x\left(E^n_{z(i+1,j,k-1)}-E^n_{z(i,j,k-1)}\right)\right] \\
& -H^{n-\frac{1}{2}}_{z(i,j,k-1)}\left[b_x\left(E^n_{y(i+1,j,k-1)}-E^n_{y(i,j,k-1)}\right) - b_y\left(E^n_{x(i,j+1,k-1)}-E^n_{x(i,j,k-1)}\right)\right] \\
& + \sum_{r=x,y,z}\left(\varepsilon_{r(i,j-1,k)}(E^n_{r(i,j-1,k)})^2 + 4\cdot\frac{1}{4}\mu(H^{n-\frac{1}{2}}_{r(i,j-1,k)})^2\right) \\
& -H^{n-\frac{1}{2}}_{x(i,j-1,k)}\left[b_y\left(E^n_{z(i,j,k)}-E^n_{z(i,j-1,k)}\right) - b_z\left(E^n_{y(i,j-1,k+1)}-E^n_{y(i,j-1,k)}\right)\right] \\
& -H^{n-\frac{1}{2}}_{y(i,j-1,k)}\left[b_z\left(E^n_{x(i,j-1,k+1)}-E^n_{x(i,j-1,k)}\right) - b_x\left(E^n_{z(i+1,j-1,k)}-E^n_{z(i,j-1,k)}\right)\right] \\
& -H^{n-\frac{1}{2}}_{z(i,j-1,k)}\left[b_x\left(E^n_{y(i+1,j-1,k)}-E^n_{y(i,j-1,k)}\right) - b_y\left(E^n_{x(i,j,k)}-E^n_{x(i,j-1,k)}\right)\right] \\
& + \cdots\cdots\Bigg\}
\end{aligned}
\tag{A16}
$$

In (A16), the justification for writing the H components as $4\cdot\frac{1}{4}\mu(H^{n-\frac{1}{2}}_{r(i,j,k)})^2$, $(r=x,y,z)$ is because each H component is surrounded

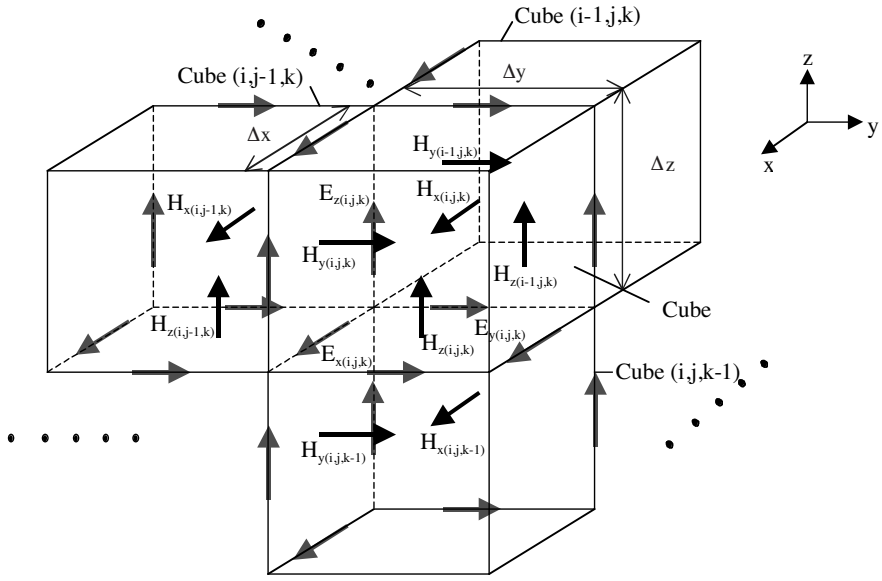

Figure A2. Four adjacent cubes.

or 'shared' by four other E field components, as seen in Figure A2. Also we want each group to center around an E field component. So the H field component has to be divided into four parts, each part is associated with an adjacent E field. Collecting and regrouping the terms in (A16) around $E^n_{x(i,j,k)}$, $E^n_{y(i,j,k)}$, $E^n_{z(i,j,k)}$:

$$
\begin{aligned}
V^n = {} & \cdots\cdots + \\
& \frac{\Delta V}{2}\left\{\begin{array}{l}
\varepsilon_{x(i,j,k)}(E^n_{x(i,j,k)})^2 + \dfrac{1}{4}\mu(H^{n-\frac{1}{2}}_{y(i,j,k)})^2 \\
+\dfrac{1}{4}\mu(H^{n-\frac{1}{2}}_{y(i,j,k-1)})^2 + \dfrac{1}{4}\mu(H^{n-\frac{1}{2}}_{z(i,j,k)})^2 + \dfrac{1}{4}\mu(H^{n-\frac{1}{2}}_{z(i,j-1,k)})^2 \\
+E^n_{x(i,j,k)}\left[b_z\left(H^{n-\frac{1}{2}}_{y(i,j,k)} - H^{n-\frac{1}{2}}_{y(i,j,k-1)}\right) - b_y\left(H^{n-\frac{1}{2}}_{z(i,j,k)} - H^{n-\frac{1}{2}}_{z(i,j-1,k)}\right)\right]
\end{array}\right\} \\
& + \frac{\Delta V}{2}\left\{\begin{array}{l}
\varepsilon_{y(i,j,k)}(E^n_{y(i,j,k)})^2 + \dfrac{1}{4}\mu(H^{n-\frac{1}{2}}_{x(i,j,k)})^2 \\
+\dfrac{1}{4}\mu(H^{n-\frac{1}{2}}_{x(i,j,k-1)})^2 + \dfrac{1}{4}\mu(H^{n-\frac{1}{2}}_{z(i,j,k)})^2 + \dfrac{1}{4}\mu(H^{n-\frac{1}{2}}_{z(i-1,j,k)})^2 \\
+E^n_{y(i,j,k)}\left[b_x\left(H^{n-\frac{1}{2}}_{z(i,j,k)} - H^{n-\frac{1}{2}}_{z(i-1,j,k)}\right) - b_z\left(H^{n-\frac{1}{2}}_{x(i,j,k)} - H^{n-\frac{1}{2}}_{x(i,j,k-1)}\right)\right]
\end{array}\right\}
\end{aligned}
$$

$$+\frac{\Delta V}{2}\left\{\begin{array}{l}\varepsilon_{z(i,j,k)}(E^n_{z(i,j,k)})^2+\frac{1}{4}\mu(H^{n-\frac{1}{2}}_{x(i,j,k)})^2\\ +\frac{1}{4}\mu(H^{n-\frac{1}{2}}_{x(i,j-1,k)})^2+\frac{1}{4}\mu(H^{n-\frac{1}{2}}_{y(i,j,k)})^2+\frac{1}{4}\mu(H^{n-\frac{1}{2}}_{y(i-1,j,k)})^2\\ +E^n_{z(i,j,k)}\left[b_y\left(H^{n-\frac{1}{2}}_{x(i,j,k)}-H^{n-\frac{1}{2}}_{x(i,j-1,k)}\right)-b_x\left(H^{n-\frac{1}{2}}_{y(i,j,k)}-H^{n-\frac{1}{2}}_{y(i-1,j,k)}\right)\right]\end{array}\right\}$$
$$+\cdots \quad \text{(A17)}$$

In writing (A17) some irrelevant terms from (A16) have been excluded. Each expression in the braces is a group. Call the first group V^n_{xs} since its associated E field is along x axis, s is an integer enumerating the E field index (i, j, k). Proceeding to group according to all E fields in the model, (A17) can be written as:

$$V^n = \Delta V\left(\sum_s V^n_{xs}+\sum_s V^n_{ys}+\sum_s V^n_{zs}\right), \quad s=1,2,3,\ldots \qquad \text{(A18)}$$

By showing that each V^n_{xs}, V^n_{ys}, V^n_{zs} is positive definite, then V^n is also positive definite. Suppose we consider one of the groups centering on E_z component. Writing this as:

$$\begin{aligned}V_z &= \varepsilon E_1^2+\frac{1}{4}\mu H_3^2+\frac{1}{4}\mu H_1^2+\frac{1}{4}\mu H_2^2+\frac{1}{4}\mu H_4^2\\ &\quad +E_1[b_y(H_3-H_1)-b_x(H_2-H_4)]\\ &= [E_1 \quad H_1 \quad H_2 \quad H_3 \quad H_4]^T\begin{bmatrix}\varepsilon & -\frac{1}{2}b_y & -\frac{1}{2}b_x & \frac{1}{2}b_y & \frac{1}{2}b_x\\ -\frac{1}{2}b_y & \frac{1}{4}\mu & 0 & 0 & 0\\ -\frac{1}{2}b_x & 0 & \frac{1}{4}\mu & 0 & 0\\ \frac{1}{2}b_y & 0 & 0 & \frac{1}{4}\mu & 0\\ \frac{1}{2}b_x & 0 & 0 & 0 & \frac{1}{4}\mu\end{bmatrix}\begin{bmatrix}E_1\\ H_1\\ H_2\\ H_3\\ H_4\end{bmatrix}\\ &= \overline{x}^T\overline{\overline{A}}\overline{x} \qquad \text{(A19)}\end{aligned}$$

Equation (A19) is only applicable for interior cells, i.e., when the cell is not a boundary cell. In general to include boundary cells, the matrix $\overline{\overline{A}}$ should be generalized as:

$$\overline{\overline{A}} = \begin{bmatrix}\varepsilon & -\frac{1}{2}b_y & -\frac{1}{2}b_x & \frac{1}{2}b_y & \frac{1}{2}b_x\\ -\frac{1}{2}b_y & a_1^2\mu & 0 & 0 & 0\\ -\frac{1}{2}b_x & 0 & a_1^2\mu & 0 & 0\\ \frac{1}{2}b_y & 0 & 0 & a_3^2\mu & 0\\ \frac{1}{2}b_x & 0 & 0 & 0 & a_4^2\mu\end{bmatrix} \qquad \text{(A20)}$$

Where $a_i \in \{\frac{1}{\sqrt{2}}, \frac{1}{\sqrt{3}}, \frac{1}{\sqrt{4}}\}$, $i = 1, 2, 3, 4$. The coefficient a_i assumes these values because at the boundary cell a H field component is surrounded by two to three E field components only. This condition is illustrated in Figure A3.

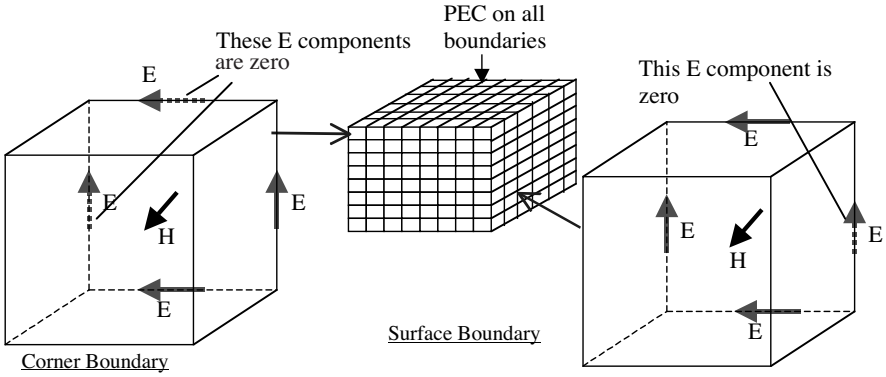

Figure A3. H field components at surface boundary and corner boundary.

For V_z to be positive definite, the matrix $\overline{\overline{A}}$ of (A20) must fulfils the Sylvester's Criterion for positive definiteness. There are 5 principal minors $P_1, P_2 \ldots, P_5$. We begin by computing the principal minors P_1 and insisting that it is greater than zero, then repeating this for the other principal minors. It is implicitly assumed that $\mu > 0$.

$$P_1 = \varepsilon > 0 \Rightarrow \varepsilon > 0 \tag{A21a}$$

$$P_2 = \begin{vmatrix} \varepsilon & -\frac{1}{2}b_y \\ -\frac{1}{2}b_y & a_1^2\mu \end{vmatrix} = a_1^2\mu\varepsilon - \frac{1}{4}b_y^2 > 0 \Rightarrow \mu\varepsilon > \frac{1}{(2a_1)^2}b_y^2$$

$$\text{Using} \quad b_y = \frac{\Delta t}{\Delta y} \text{ and } c = \frac{1}{\sqrt{\mu\varepsilon}} \Rightarrow \Delta t < \frac{1}{c\sqrt{\frac{1}{(2a_1\Delta y)^2}}} \tag{A21b}$$

$$\begin{aligned} P_3 &= \begin{vmatrix} \varepsilon & -\frac{1}{2}b_y & -\frac{1}{2}b_x \\ -\frac{1}{2}b_y & a_1^2\mu & 0 \\ -\frac{1}{2}b_x & 0 & a_2^2\mu \end{vmatrix} \\ &= (a_1a_2\mu)^2\varepsilon - \frac{\mu}{4}(a_1b_x)^2 - \frac{\mu}{4}(a_2b_y)^2 > 0 \\ &\Rightarrow \mu\varepsilon > \left(\frac{b_x}{2a_2}\right)^2 + \left(\frac{b_y}{2a_1}\right)^2 \end{aligned}$$

$$\Rightarrow \Delta t < \frac{1}{c\sqrt{\dfrac{1}{(2a_2\Delta x)^2}+\dfrac{1}{(2a_1\Delta y)^2}}} \tag{A21c}$$

$$P_4 = \begin{bmatrix} \varepsilon & -\frac{1}{2}b_y & -\frac{1}{2}b_x & \frac{1}{2}b_y \\ -\frac{1}{2}b_y & a_1^2\mu & 0 & 0 \\ -\frac{1}{2}b_x & 0 & a_2^2\mu & 0 \\ \frac{1}{2}b_y & 0 & 0 & a_3^2\mu \end{bmatrix}$$

$$= (-1)^{1+4}\left(\frac{1}{2}b_y\right)\begin{vmatrix} -\frac{1}{2}b_y & a_1^2\mu & 0 \\ -\frac{1}{2}b_x & 0 & a_2^2\mu \\ \frac{1}{2}b_y & 0 & 0 \end{vmatrix} + (-1)^{4+4}a_3^2\mu P_3 > 0$$

$$\Rightarrow -\left(\frac{a_1a_2}{2}\mu b_y\right)^2 + \left(a_3^2\mu\right)P_3 > 0$$

$$\Rightarrow \mu\varepsilon > \left(\frac{b_x}{2a_2}\right)^2 + \left(\frac{b_y}{2a_1}\right)^2 + \left(\frac{b_y}{2a_3}\right)^2$$

$$\Rightarrow \Delta t < \frac{1}{c\sqrt{\dfrac{1}{(2a_2\Delta x)^2}+\dfrac{1}{\left(2\dfrac{a_1a_3}{\sqrt{a_1^2+a_3^2}}\right)^2\Delta y^2}}} \tag{A21d}$$

$$P_5 = \begin{vmatrix} \varepsilon & -\frac{1}{2}b_y & -\frac{1}{2}b_x & \frac{1}{2}b_y & \frac{1}{2}b_x \\ -\frac{1}{2}b_y & a_1^2\mu & 0 & 0 & 0 \\ -\frac{1}{2}b_x & 0 & a_2^2\mu & 0 & 0 \\ \frac{1}{2}b_y & 0 & 0 & a_3^2\mu & 0 \\ \frac{1}{2}b_x & 0 & 0 & 0 & a_4^2\mu \end{vmatrix}$$

$$= (-1)^{1+5}\left(\frac{1}{2}b_x\right)\begin{vmatrix} -\frac{1}{2}b_y & a_1^2\mu & 0 & 0 \\ -\frac{1}{2}b_x & 0 & a_2^2\mu & 0 \\ \frac{1}{2}b_y & 0 & 0 & a_3^2\mu \\ \frac{1}{2}b_x & 0 & 0 & 0 \end{vmatrix} + (-1)^{5+5}a_4^2\mu P_4 > 0$$

$$\Rightarrow \mu\varepsilon > \left(\frac{b_x}{2a_2}\right)^2 + \left(\frac{b_x}{2a_4}\right)^2 + \left(\frac{b_y}{2a_1}\right)^2 + \left(\frac{b_y}{2a_3}\right)^2$$

$$\Rightarrow \Delta t < \frac{1}{c\sqrt{\dfrac{1}{\left(\dfrac{2a_2a_4}{\sqrt{a_2^2+a_4^2}}\right)^2\Delta x^2}+\dfrac{1}{\left(\dfrac{2a_1a_3}{\sqrt{a_1^2+a_3^2}}\right)^2\Delta y^2}}} \tag{A21e}$$

Table A1. Computation of coefficient for Δx and Δy.

a_1 or a_2	a_3 or a_4	$\frac{2a_1a_3}{\sqrt{a_1^2+a_3^2}}$ or $\frac{2a_2a_4}{\sqrt{a_2^2+a_4^2}}$	a_i $i=1,2,3,4$	$2a_i$
$1/\sqrt{4}$	$1/\sqrt{4}$	$1/\sqrt{2} \cong 0.70711$	$1/\sqrt{4}$	2
$1/\sqrt{4}$	$1/\sqrt{3}$	$1/\sqrt{7} \cong 0.75593$	$1/\sqrt{3}$	$2/\sqrt{3} \cong 1.15470$
$1/\sqrt{4}$	$1/\sqrt{2}$	$2/\sqrt{6} \cong 0.81650$	$1/\sqrt{2}$	$2/\sqrt{2} \cong 1.41421$
$1/\sqrt{3}$	$1/\sqrt{3}$	$2/\sqrt{6} \cong 0.81650$		
$1/\sqrt{3}$	$1/\sqrt{2}$	$2/\sqrt{5} \cong 0.89443$		
$1/\sqrt{2}$	$1/\sqrt{2}$	1		

From (A21a) to (A21e), we see that $\mu > 0$, $\varepsilon > 0$ and Δt needs to be smaller than a certain limit. The smallest limit from (A21b) to (A21e) for all combination of a_1, a_2, a_3 and a_4 will be taken as the constraint for Δt. Table A1 shows the values for the coefficient of Δx and Δy for different combinations of a_1, a_2, a_3 and a_4.

Consider the expression:

$$\frac{1}{\sqrt{\frac{1}{(c_1\Delta x)^2}+\frac{1}{(c_2\Delta y)^2}}} = \frac{1}{\sqrt{\frac{1}{c_1^2}\left(\frac{1}{\Delta x^2}\right)+\frac{1}{c_2^2}\left(\frac{1}{\Delta y^2}\right)}}$$

The smallest value is obtained when the denominator is maximum. If Δx and Δy are fixed, then c_1 and c_2 must be as small as possible. Using Table A1, we observe that:

$$\begin{aligned}
&\frac{1}{\sqrt{\frac{1}{(2a_1\Delta y)^2}}} > \frac{1}{\sqrt{\frac{1}{(2a_2\Delta x)^2}+\frac{1}{(2a_1\Delta y)^2}}} \\
&> \frac{1}{\sqrt{\frac{1}{(2a_2\Delta x)^2}+\frac{1}{\left(\frac{2a_1a_3\Delta y}{\sqrt{a_1+a_3}}\right)^2}}} > \frac{1}{\sqrt{\frac{1}{\left(\frac{2a_2a_4\Delta x}{\sqrt{a_2^2+a_2^4}}\right)^2}+\frac{1}{\left(\frac{2a_1a_3\Delta y}{\sqrt{a_1+a_3}}\right)^2}}}
\end{aligned} \tag{A22}$$

Also from Table A1, we observe that $\frac{2a_1a_3}{\sqrt{a_1^2+a_3^2}}$ and $\frac{2a_2a_4}{\sqrt{a_2^2+a_4^2}}$ are smallest when $a_1 = a_3 = a_2 = a_4 = \frac{1}{\sqrt{4}}$. The corresponding coefficients for Δx

and Δy are $\frac{1}{\sqrt{2}}$. We conclude that if Δt satisfies:

$$\Delta t < \frac{1}{c\sqrt{\dfrac{1}{\left(\frac{1}{\sqrt{2}}\right)^2\Delta x^2} + \dfrac{1}{\left(\frac{1}{\sqrt{2}}\right)^2\Delta y^2}}} = \frac{1}{c\sqrt{2}\sqrt{\dfrac{1}{\Delta x^2} + \dfrac{1}{\Delta y^2}}},$$

$$c = \frac{1}{\sqrt{\mu\varepsilon}} \quad \text{(A23a)}$$

Then all conditions of (A21b) to (A21e) will be fulfilled and V_z will be positive definite. This procedure can also be applied to V_x and V_y, whose details would not be provided:

$$\text{For } V_x: \ \Delta t < \frac{1}{c\sqrt{2}\sqrt{\dfrac{1}{\Delta y^2} + \dfrac{1}{\Delta z^2}}} \quad \text{For } V_y: \ \Delta t < \frac{1}{c\sqrt{2}\sqrt{\dfrac{1}{\Delta x^2} + \dfrac{1}{\Delta z^2}}} \quad \text{(A23b)}$$

Equations (A23a) and (A23b) apply to a single cell. To ensure that all groups V_{xs}^n, V_{ys}^n and V_{zs}^n, $s \in \{1, 2, 3 \dots\}$, in the 3D model are positive definite, these need to be enforced for every cell. This requirement can be summarized as follows:

For a 3D FDTD model according to Yee's formulation, suppose the followings apply:

1. Update equations for E and H field components are given by the Canonical FDTD Form (1a) to (1f).
2. Boundaries of the model are perfect electric conductor (PEC).
3. All cubes are similar in size with edges Δx, Δy and Δz.

Then for all $i \in \{1, 2, \dots, n_x\}$, $j \in \{1, 2, \dots, n_y\}$, $k \in \{1, 2, \dots, n_z\}$, $\Delta V = \Delta x \Delta y \Delta z$, the function:

$$V^n = \frac{\Delta V}{2} \sum_{k=1}^{n_z} \sum_{j=1}^{n_y} \sum_{i=1}^{n_x} \left[\sum_{r=x,y,z} \left(\varepsilon_{r(i,j,k)} (E_{r(i,j,k)}^n)^2 + \mu (H_{r(i,j,k)}^{n-\frac{1}{2}})^2 \right) - \Delta t \left(H^{n-\frac{1}{2}} \cdot \nabla \times E^n \right)_{(i,j,k)} \right]$$

is positive definite if and only if:

- $\varepsilon_{x(i,j,k)} > 0$, $\varepsilon_{y(i,j,k)} > 0$, $\varepsilon_{z(i,j,k)} > 0$ and $\mu > 0$.
- For $\varepsilon = \min\{\varepsilon_{x(i,j,k)}, \varepsilon_{y(i,j,k)}, \varepsilon_{z(i,j,k)}\}$ and $c_m = \frac{1}{\sqrt{\mu\varepsilon}}$, let:

$$\Delta t < \min\left\{ \frac{1}{c_m\sqrt{2}\sqrt{\frac{1}{\Delta y^2}+\frac{1}{\Delta z^2}}}, \frac{1}{c_m\sqrt{2}\sqrt{\frac{1}{\Delta x^2}+\frac{1}{\Delta z^2}}}, \frac{1}{c_m\sqrt{2}\sqrt{\frac{1}{\Delta x^2}+\frac{1}{\Delta y^2}}} \right\}$$

This proves Lemma 2.2.

APPENDIX B. STABILITY FOR 3D FDTD MODEL

We now prove Theorem 2.3. Suppose a FDTD framework satisfies all the conditions of Lemma 2.1 and 2.2. Since V^n is positive definite, it can be written in the form [16]:

$$V^n = \overline{X}^T \overline{\overline{P}}\, \overline{X}, \qquad \overline{X} \in R^M \tag{B1}$$

where M is as given by (5b) and $\overline{\overline{P}}$ is a square symmetric matrix of order M. Superscript T represents matrix transposition. Introducing the linear transformation $\overline{X} = \overline{\overline{Q}}\,\overline{Y}$:

$$V^n = \overline{Y}^T \left(\overline{\overline{Q}}^T \overline{\overline{P}}\, \overline{\overline{Q}} \right) \overline{Y} \tag{B2}$$

The matrix transformation $\overline{\overline{Q}}^T \overline{\overline{P}}\, \overline{\overline{Q}}$ of (B2) is a special form of Similarity Transformation known as Congruence Transformation [16]. Since matrix $\overline{\overline{P}}$ is positive definite, from linear algebra we know that a nonsingular matrix $\overline{\overline{Q}}$ exists such that [16, chapter 3]:

$$\overline{\overline{Q}}^T \overline{\overline{P}}\, \overline{\overline{Q}} = diag(1, 1, 1, \ldots, 1)$$

Thus

$$V^n = \overline{Y}^T \left(\overline{\overline{Q}}^T \overline{\overline{P}}\, \overline{\overline{Q}} \right) \overline{Y} = \overline{\overline{Y}}^T \overline{\overline{Y}} = y_1^2 + y_2^2 + y_3^2 + \cdots + y_M^2 \tag{B3}$$

Taking an arbitrary norm for $\overline{Y} = \overline{\overline{Q}}^{-1} \overline{X}$:

$$\left\| \overline{Y} \right\| = \left\| \overline{\overline{Q}}^{-1} \overline{X} \right\| \leq \left\| \overline{\overline{Q}}^{-1} \right\| \left\| \overline{X} \right\| \tag{B4}$$

Where $\left\| \overline{\overline{Q}}^{-1} \right\|$ is a finite positive value called the matrix or operator norm as defined in [16, chapter 2]. We thus have the following implication from (B4):

$$\left\| \overline{Y} \right\| \to \infty \Rightarrow \left\| \overline{X} \right\| \to \infty \tag{B5}$$

Observe that from (B3), $V^n = \overline{X}^T \overline{\overline{P}}\, \overline{X} = \overline{Y}^T \overline{Y}$ is radially unbounded [13, chapter 3] in relation to elements of $\overline{Y}$. This means that if V^n approaches infinity, at least one of the elements of $\overline{Y}$ must also approaches infinity. Suppose we use the L_2 vector norm:

$$\left\|\overline{X}\right\| = \left(x_1^2 + x_2^2 + \cdots x_M^2\right)^{\frac{1}{2}} \text{ and } \left\|\overline{Y}\right\| = \left(y_1^2 + y_2^2 + \cdots + y_M^2\right)^{\frac{1}{2}} \tag{B6}$$

Using (B5) we note that V^n is also radially unbounded in relation to elements of $\overline{X}$. This implies that if V^n is bounded, all the elements in $\overline{X}$ must also be finite, i.e., all the E and H field components are finite. For V^n to be bounded for $n = 1, 2, 3, \ldots$, a sufficient condition is P_d be negative or zero. This completes the proof. □

APPENDIX C. NEGATIVE REGION FOR RESISTIVE VOLTAGE SOURCE

We first note from [2] that to derive equation (17) the current of a resistive voltage source is:

$$I_s^{n+\frac{1}{2}} = \frac{\Delta t}{2R_s}\left(E_z^n + E_z^{n+1}\right) + \frac{V_s^{n+\frac{1}{2}}}{R_s} \tag{C1}$$

From $\nabla \times \tilde{H} = \tilde{J} + \varepsilon \frac{\partial \tilde{E}}{\partial t}$ and using center difference scheme according to Yee's formulation [3], concentrating on z component of E field at (i, j, k) (assuming the source to coincide with $E_{z(i,j,k)}$):

$$\nabla \times H_{z(i,j,k)}^{n+\frac{1}{2}} = \frac{I_s^{n+\frac{1}{2}}}{\Delta x \Delta y} + \frac{\varepsilon}{\Delta t}\left(E_{z(i,j,k)}^{n+1} + E_{z(i,j,k)}^{n}\right) \tag{C2}$$

Let $V_s^{n+\frac{1}{2}}$ be a constant, called it V_{so} and limiting the maximum source current to $I_{s(\max)} = \frac{V_{so}}{R_s}$. Let us also introduce the notations $x = E_{z(i,j,k)}^n$, $x^{n+1} = E_{z(i,j,k)}^{n+1}$, $y = \nabla \times H_{z(i,j,k)}^{n+\frac{1}{2}}$, $v = \frac{V_{so}}{\Delta z}$. Then from (C2):

$$\begin{aligned} &\frac{\Delta t}{\varepsilon} \nabla \times H_{z(i,j,k)}^{n+\frac{1}{2}} - \left(E_{z(i,j,k)}^{n+1} + E_{z(i,j,k)}^{n}\right) \\ &= \frac{\Delta t I_s^{n+\frac{1}{2}}}{\varepsilon \Delta x \Delta y} < 2 \frac{\Delta t \Delta z}{2\varepsilon \Delta x \Delta y \Delta z} \cdot \frac{V_{so}}{R_s} = 2 D_z v \\ &\Rightarrow y < \frac{2\varepsilon}{\Delta t} D_z v + \frac{\varepsilon}{\Delta t}\left(x^{n+1} - x\right) \end{aligned} \tag{C3}$$

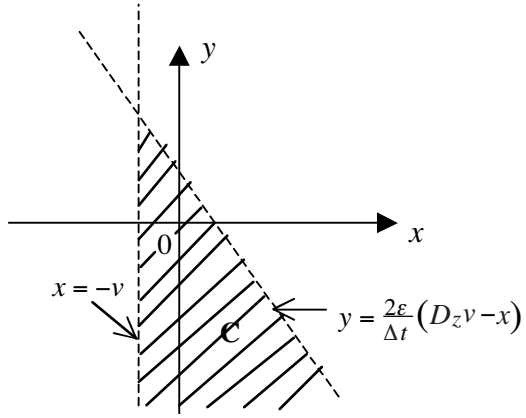

Figure C1. Intersection of $D^{n+\frac{1}{2}}(x, y, v) \leq 0$ and $y < \frac{2\varepsilon}{\Delta t}(D_z v - x)$.

Substituting (17) for $x^{n+1} = E^{n+1}_{z(i,j,k)}$ into inequality (C3), and performing some algebra:

$$y < \frac{2\varepsilon}{\Delta t} D_z v + \frac{\varepsilon}{\Delta t} \frac{1}{1 + D_z} \left(\frac{\Delta t}{\varepsilon} y - 2D_z(x + v) \right)$$
$$\Rightarrow y < \frac{2\varepsilon}{\Delta t}(D_z v - x) \tag{C4}$$

The intersection of region described by (C4) and region **A** of Figure 5 is shown in Figure C1. We call this region **C**. From Figure C1, we notice that in order for the resistive voltage source to be continuously supplying energy to the model, the new value for $x^{n+1} = E^{n+1}_{z(i,j,k)}$ must be greater than $-v$. Otherwise there is no chance the elemental dissipation can be negative. Thus enforcing this requirement from (17):

$$x^{n+1} = \frac{1 - D_z}{1 + D_z} x + \frac{\Delta t}{\varepsilon(1 + D_z)} y - \frac{2D_z}{1 + D_z} v > -v$$
$$\Rightarrow y > -\frac{\varepsilon}{\Delta t}(1 - D_z)(x + v) \tag{C5}$$

(C4), (C5) and $D^{n+\frac{1}{2}}(x, y, v) \leq 0$ corresponds to the (20a)–(20c). Using these inequalities, the region of Figure 6a can be generated for $D_z < 1$. Inequality (C5) will degenerate to $y = 0$ when $D_z > 1$, allowing us to generate Figure 6b. □

REFERENCES

1. Yee, K. S., "Numerical solution of initial boundary value problems involving Maxwell's equations in isotropic media," *IEEE Trans. Antennas and Propagation*, Vol. 14, 302–307, May 1966.
2. Piket-May, M. J., A. Taflove, and J. Baron, "FD-TD modeling of digital signal propagation in 3-D circuits with passive and active loads," *IEEE Trans. Microwave Theory and Techniques*, Vol. 42, 1514–1523, August 1994.
3. Taflove, A., *Computational Electrodynamics — The finite-difference time-domain method*, Artech House, 1995.
4. Kung, F. and H. T. Chuah, "Modeling a diode in FDTD," *J. of Electromagnetic Waves and Appl.*, Vol. 16, No. 1, 99–110, 2002.
5. Kung, F. and H. T. Chuah, "Modeling of bipolar junction transistor in FDTD simulation of printed circuit board," *Progress in Electromagnetic Research*, PIER 36, 179–192, 2002.
6. Pereda, J. A., L. A. Vielva, A. Vegas, et al., "Analyzing the stability of the FDTD technique by combining the von Neumann method with the Routh-Hurwitz criterion," *IEEE Trans. Microwave Theory and Techniques*, Vol. 49, 377–381, Feb. 2001.
7. Thiel, W. and L. P. B. Katehi, "Some aspects of stability and numerical dissipation of the finite-difference time-domain (FDTD) technique including passive and active lumped-elements," *IEEE Trans. Microwave Theory and Techniques*, Vol. 50, 2159–2165, Sep. 2002.
8. Remis, R. F., "On the stability of the finite-difference time-domain method," *J. of Computational Physics*, Vol. 163, No. 1, 249–261, Sep. 2000.
9. Strikwerda, J. C., *Finite Difference Schemes and Partial Differential Equations*, Wadsworth & Brooks/Cole Mathematics Series, 1989.
10. Scheinerman, E. R., *Invitation to Dynamical Systems*, Prentice Hall, 1996.
11. Elaydi, S. N., *Discrete Chaos*, Chapman & Hall/CRC, 2000.
12. Merkin, D. R., *Introduction to the Theory of Stability*, Springer-Verlag, 1997.
13. Khalil, H. K., *Nonlinear Systems*, 2nd edition, Prentice Hall, 1996.
14. James, G., *Advance Modern Engineering Mathematics*, Addison-Wesley, 1993.
15. "Surface mount RF Schottky barrier diodes: HSMS-

282x series," Technical Data, Agilent Technologies Inc., www.semiconductor.agilent.com, 2000.

16. Ortega, J. M., *Matrix Theory — A second course*, Plenum Press, 1987.